NASA TM X-768

TECHNICAL MEMORANDUM

X-768

THE TRANSONIC LONGITUDINAL AND LATERAL AERODYNAMIC CHARACTERISTICS OF A LOW-FINENESS-RATIO ELLIPTIC HYPERSONIC CONFIGURATION EMPLOYING VARIABLE-SWEEP WING PANELS FOR IMPROVING SUBSONIC LIFT AND PERFORMANCE

By Bernard Spencer, Jr., Beverly Z. Henry, Jr., and Lawrence E. Putnam

Langley Research Center
Langley Station, Hampton, Va.

NATIONAL AERONAUTICS AND SPACE ADMINISTRATION

WASHINGTON

March 1963

NATIONAL AERONAUTICS AND SPACE ADMINISTRATION

TECHNICAL MEMORANDUM X-768

THE TRANSONIC LONGITUDINAL AND LATERAL AERODYNAMIC CHARACTERISTICS OF A LOW-FINENESS-RATIO ELLIPTIC HYPERSONIC CONFIGURATION EMPLOYING VARIABLE-SWEEP WING PANELS FOR IMPROVING SUBSONIC LIFT AND PERFORMANCE*

By Bernard Spencer, Jr., Beverly Z. Henry, Jr., and Lawrence E. Putnam

SUMMARY

An investigation has been conducted in the Langley 7- by 10-foot transonic tunnel at Mach numbers from 0.40 to 1.14 on the longitudinal and lateral aerodynamic characteristics of an elliptic body with a ratio of the major-to-minor axes of 2.0 and with variable-sweep wing panels located on the upper surface. The wing-panel pivot point was located at 65.5 percent of the body length. Longitudinal control for the configuration was provided by use of a flap located at the base of the body.

Results of the investigation indicated that at a Mach number of 0.40 extension of the wing panel from a fully retracted position to a leading-edge sweep of 0° increased the untrimmed maximum lift-drag ratio from approximately 1.95 to 6.10, increased the lift-curve slope from 0.0070 to 0.0360, and caused a rearward shift in the center of pressure of approximately 10 percent of the body length. Extension of the wing panels from a fully retracted position to 60° resulted in an increase in maximum lift-drag ratio from approximately 2.2 to 4.3 at a Mach number of 1.0.

The configuration exhibited directional instability for all angles of attack and wing-panel sweeps tested at Mach numbers of 0.40 and 0.60. However, the configuration having a wing-panel sweep of 60° was directionally stable at the higher angles of attack in the Mach number range from 0.80 to 1.14. The configuration had positive effective dihedral for all wing-panel sweeps and Mach numbers tested.

*Title Unclassified.

INTRODUCTION

The National Aeronautics and Space Administration is currently conducting general research programs to determine the aerodynamic characteristics associated with reentry configurations capable of producing lift and moderate values of lift-drag ratio from hypersonic to low subsonic speeds. Previous investigations have indicated the advantages in maneuverability, range control, heating rates, and reentry corridor width of the lifting type of reentry configuration as compared with the nonlifting vehicle. (See refs. 1 to 4.) Numerous configurations of the lifting type have been investigated from hypersonic to low subsonic speeds. (See, e.g., refs. 5 to 9.) Configurations designed for moderate values of lift and lift-drag ratios to provide good hypersonic aerodynamic and heating characteristics exhibit poor landing qualities due to the resultant low values of subsonic lift-curve slope and lift-drag ratios.

Considerable improvement in the transonic to low subsonic performance and lifting capabilities for a right triangular pyramidal reentry vehicle which has been shown to have satisfactory longitudinal and lateral stability characteristics from hypersonic to low subsonic speeds (refs. 10 to 14) was realized by use of variable-sweep wing panels located on the upper surface of the configuration. (See ref. 15.) This configuration also had little or no change in longitudinal stability level between the fully retracted wing-panel configuration at a Mach number of 1.10 and the 0° leading-edge sweep of the fully extended wing panel at a Mach number of 0.40. Losses in lift at moderate angles of attack for leading-edge sweep angles below 40°, however, restricted the high lift capability for the configuration with the lowest sweep and maximum lift-drag ratio. Also, because of the body triangular cross section, usable internal volume was restricted; at extreme altitudes it would be somewhat difficult to pressurize this triangular cross section. When usable volume and pressurization are factors to be considered, a configuration having a more nearly circular cross section, yet still maintaining the hypersonic to subsonic lateral and longitudinal stability characteristics of the pyramidal type of configuration, is more desirable.

The present study was initiated, therefore, as a preliminary investigation to determine the longitudinal and lateral stability and control characteristics of a low-fineness-ratio body having an elliptic cross section and a ratio of the major-to-minor axes of 2.0. These factors should provide a more compact configuration having better usable volume distribution than the pyramidal type of configuration. Variable-sweep wing panels were located on the upper surface of the configuration in order to improve lift and performance at transonic and low subsonic speeds. (See also ref. 15.) The airfoil section of the present wing panel, however, was a highly cambered airfoil with a higher maximum lift than that obtained from the airfoil used in the investigation described in reference 15. This airfoil was employed in an effort to improve the high lift characteristics of the low-sweep landing configuration.

SYMBOLS

All data presented herein are referenced to the body-axis system, except the lift and drag which are referenced to the stability-axis system. All coefficients

are nondimensionalized with respect to the theoretical projected planform area, the theoretical length (fig. 1), and the span of the basic body (wing panels fully retracted). The moment reference point is located 13.07 inches aft of the theoretical body apex, corresponding to 65.5 percent of the theoretical body length, and is the longitudinal location of the pivot point for the variable-sweep wing panels. The location of the moment reference point was determined from weight and balance considerations for the vehicle in the unpowered reentry and landing configuration.

A body aspect ratio, $\frac{b^2}{S}$, 0.421

b body span, 0.4698 ft

C_D drag coefficient, $\frac{\text{Drag}}{qS}$

C_L lift coefficient, $\frac{\text{Lift}}{qS}$

C_{L_α} lift-curve slope, per deg

C_l rolling-moment coefficient, $\frac{\text{Rolling moment}}{qSb}$

C_m pitching-moment coefficient, $\frac{\text{Pitching moment}}{qSc}$

$\frac{\partial C_m}{\partial C_L}$ longitudinal stability parameter

$C_{m_{\delta_f}}$ longitudinal-control effectiveness parameter

C_n yawing-moment coefficient, $\frac{\text{Yawing moment}}{qSb}$

$C_{p,b}$ base pressure coefficient

C_Y side-force coefficient, $\frac{\text{Side force}}{qS}$

c theoretical body length, 1.667 ft

L/D lift-drag ratio

M Mach number

q dynamic pressure, lb/sq ft

S theoretical projected body planform area, 0.5216 sq ft

x longitudinal body coordinate

y lateral body coordinate

z vertical body coordinate

$C_{l_\beta} = \frac{\partial C_l}{\partial \beta}$ through $\beta \approx 0$, per deg

$C_{n_\beta} = \frac{\partial C_n}{\partial \beta}$ through $\beta \approx 0$, per deg

$C_{Y_\beta} = \frac{\partial C_Y}{\partial \beta}$ through $\beta \approx 0$, per deg

α angle of attack, deg

β angle of sideslip, deg

δ_f deflection of flap located at body base, positive when trailing edge down, deg

Λ_{LE} wing-panel leading-edge sweep, deg

Subscript:

max maximum

MODEL

The basic body of the present investigation has the wing panels fully retracted ($\Lambda_{LE} = 90^\circ$) and is without the control flap located at the body base. The body has a modified elliptic cross section with a ratio of the major-to-minor axes of 2.0 and with each local cross section displaced below the reference line. (See fig. 1.) A fairing, added to the upper surface, shields the sweeping wing panels (fig. 1) and constitutes the canopy and portion of the body located above the indicated ordinate reference line. The body contour represents a power-series body of $\frac{y}{y_{max}} = \left(\frac{x}{x_{max}}\right)^{0.5}$. Ordinates for the body as measured in the y and z directions are presented in table I for the configuration without wing panels. Photographs of the configuration without the body flap and with the wing panels at various sweep positions are presented in figure 2.

Each wing panel is a St. Cyr No. 156 (Royer) cambered airfoil section and has a taper ratio of 0.75. (Ordinates for the airfoil are presented in ref. 16.) The panels were tested at leading-edge sweep angles of 0°, 20°, 40°, 60°, and 90°.

The pivot-point location for the wing panels is the longitudinal location of the moment reference point. (See fig. 1.)

Longitudinal control was provided by use of a flap (flat plate in section) with the hinge line located at the upper surface of the model base. Flap deflections of 0°, 20°, and 40° were tested in conjunction with various wing-panel sweeps. The ratio of flap area to theoretical body-planform area was 0.066.

TESTS AND CORRECTIONS

The present investigation was conducted in the Langley 7- by 10-foot transonic wind tunnel at Mach numbers from approximately 0.40 to 1.14, corresponding to a range of average test Reynolds numbers from approximately 4.4×10^6 to approximately 7.6×10^6, based on the theoretical body length. The model was sting supported and forces and moments were measured by use of a six-component internally mounted strain-gage balance. The model was tested through an angle-of-attack range from -1° to approximately 25° at angles of sideslip of 0° and $\pm 5^\circ$. The sideslip derivatives C_{Y_β}, C_{n_β}, and C_{l_β} were obtained by measuring the slopes between $\beta = \pm 5^\circ$, taken through $\beta \approx 0^\circ$, and do not account for nonlinearities which may exist in this range of sideslip angles.

For all tests, transition was fixed by the use of No. 120 carborundum grains located at 10 percent of the body length and at 10 percent of the wing-panel chord line when the wing panels were fully extended $(\Lambda_{LE} = 0^\circ)$. Grain size was determined by the method of reference 17.

Corrections to the angle of attack due to deflection of the sting and balance under load have been applied to the data. Base pressure coefficients were measured by use of orifices at the model base and are presented as base pressure coefficients in figure 3. No corrections to the drag for the effects of base pressure have been applied to the data, however, because the configuration is considered a gliding reentry vehicle. With the use of data obtained from reference 18, an attempt has been made to assess the effects of the sting support on the drag characteristics of the configuration at the higher Mach numbers. Although no corrections to the drag have been made for sting-interference effects, maximum possible decrement in maximum lift-drag ratio appears to be approximately 5 percent. The incremental increases in lift-drag ratio realized from the extension of the wing panels, however, are unaffected by sting interference.

PRESENTATION OF RESULTS

The basic data for the configurations of this investigation are presented in the following figures:

DISCUSSION

Basic longitudinal aerodynamic characteristics of the configurations tested are presented in figures 4 to 6. A rather extensive study of the effects of extending the wing panels at various Mach numbers and of longitudinal control effectiveness are presented in these figures. Because of the preliminary nature of the configuration, only pertinent observations are made from the basic longitudinal data and from summaries of the longitudinal and lateral characteristics of the configuration as presented in figures 7 to 10.

As expected, the basic body $\left(\Lambda_{LE} = 90^\circ\right)$ had rather low values of lift and lift-curve slope at a Mach number of 0.40 (fig. 4(a)) because the body was designed for low drag and for moderate values of lift and lift-drag ratio at hypersonic speeds. Extending the wing panel from 90° to 0° at a Mach number of 0.40 increased the lift-curve slope from 0.0070 to 0.0360 and increased the untrimmed maximum lift-drag ratio from 1.95 to 6.10. (See fig. 8.) In the range of possible landing attitudes ($\alpha \approx 12^\circ$ to 16°), extending the wing panel from 90° to 0° resulted in an increase in lift coefficient from approximately 0.12 to 0.52 at $\alpha = 15^\circ$, with corresponding increases in the untrimmed lift-drag ratio from 1.9 to 4.9. (See fig. 4(a).) These combined increases in lift and lift-drag ratio should greatly enhance the landing configuration by considerable reductions in landing speed, descent rate, and ground-roll requirements. Only slight effects of increasing Mach number on C_{L_α} and $(L/D)_{max}$ for the basic body are noted. (See fig. 8.)

At $M = 0.40$ the basic body $\left(\Lambda_{LE} = 90^\circ\right)$ was statically unstable about the moment-reference location with the center-of-pressure location near 50 percent of the body length, that is, 16 percent of the body length ahead of the moment reference. Extending the wing panel from 90° to 0° caused a rearward shift of approximately 0.10c in the center-of-pressure location. As the Mach number increased

from 0.40 to 1.14, a rearward shift in the center of pressure of approximately 0.026c for the basic body occurred. (See fig. 8.)

Again at $M = 0.40$ the addition of the body-base flap to the configuration reduced the lift-curve slope for each wing-panel sweep and increased the maximum untrimmed lift-drag ratio by reducing the minimum drag of the configurations. (See figs. 5(a) and 9.) Similar results were noted in reference 15 from addition of a body-base flap. The longitudinal control effectiveness parameter $C_{m_{\delta_f}}$ for the body-base flap remains approximately constant for each wing-panel sweep and is relatively unaffected by increasing Mach number. (See fig. 10.) The effectiveness also remains essentially constant with angle of attack for each wing-panel sweep. (See fig. 5.)

The configuration exhibited directional instability for the range of angle of attack and wing-panel sweeps presented for $M = 0.40$ and 0.60. (See fig. 7.) The configuration having a wing-panel sweep of 60° was directionally stable at the higher angles of attack in the Mach number ranges from 0.80 to 1.14. This increase in directional stability occurs as a result of the rearward shift in the configuration center of pressure behind the moment reference point. Also, the effect of critical cross-flow Reynolds number at combined angles of attack and sideslip due to local velocity increases results in a reversal in side-force coefficient. An explanation of this latter effect for noncircular cross-sectional bodies is presented in reference 19.

The configuration is noted to have positive effective dihedral $-C_{l_\beta}$ for the range of leading-edge sweeps and Mach numbers tested.

SUMMARY OF RESULTS

Results of an investigation on the longitudinal and lateral aerodynamic characteristics of an elliptic body having a ratio of the major-to-minor axes of 2.0 and having variable-sweep wing panels located on the body upper surface may be summarized as follows:

Extension of the wing panel from a fully retracted position to 0° leading-edge sweep at a Mach number of 0.40 increased the untrimmed maximum lift-drag ratio from approximately 1.95 to 6.10, increased the lift-curve slope from 0.0070 to 0.0360, and effected a rearward shift in the center-of-pressure location of approximately 10 percent of the theoretical body length.

The configuration exhibited longitudinal and directional instability for all wing-panel sweeps tested at Mach numbers of 0.40 and 0.60. The configuration having a wing-panel sweep of 60° was longitudinally stable at Mach numbers greater than 0.60 and became directionally stable at the higher angles of attack in the

Mach number range from 0.80 to 1.14. The configuration had positive effective dihedral for all wing-panel sweeps and Mach numbers tested.

Langley Research Center,
National Aeronautics and Space Administration,
Langley Station, Hampton, Va., December 5, 1962.

REFERENCES

1. Becker, John V.: Re-Entry From Space. Scientific American, vol. 204, no. 1, Jan. 1961, pp. 49-57.

2. Lees, Lester, Hartwig, Frederic W., and Cohen, Clarence B.: Use of Aerodynamic Lift During Entry Into the Earth's Atmosphere. ARS Jour., vol. 29, no. 9, Sept. 1959, pp. 633-641.

3. Grant, Frederick C.: Importance of the Variation of Drag With Lift in Minimization of Satellite Entry Acceleration. NASA TN D-120, 1959.

4. Chapman, Dean R.: An Analysis of the Corridor and Guidance Requirements for Supercircular Entry into Planetary Atmospheres. NASA TR R-55, 1960.

5. Spencer, Bernard, Jr.: High-Subsonic-Speed Investigation of the Static Longitudinal Aerodynamic Characteristics of Several Delta-Wing Configurations for Angles of Attack from 0° to 90°. NASA TM X-168, 1959.

6. Hondros, James G., and Goldberg, Theodore J.: Aerodynamic Characteristics of a Group of Winged Reentry Vehicles at Mach Number 6.01 at Angles of Attack From 60° to 120° and -10° to 30° Roll at 90° Angle of Attack. NASA TM X-511, 1961.

7. Rainey, Robert W., compiler: Summary of Aerodynamic Characteristics of Low-Lift-Drag-Ratio Reentry Vehicles From Subsonic to Hypersonic Speeds. NASA TM X-588, 1961.

8. Smith, Fred M., and Nichols, Frank H., Jr.: A Wind-Tunnel Investigation of the Aerodynamic Characteristics of a Generalized Series of Winged Reentry Configurations at Angles of Attack to 180° at Mach Numbers of 2.38, 2.99 and 4.00. NASA TM X-512, 1961.

9. Allen, Clyde Q.: Low-Speed Aerodynamic Characteristics of a Model of the DS-1 Glider. NASA TM X-573, 1961.

10. Cooper, Morton, and Stainback, P. Calvin: Influence of Large Positive Dihedral on Heat Transfer to Leading Edges of Highly Swept Wings at Very High Mach Numbers. NASA MEMO 3-7-59L, 1959.

11. Paulson, John W.: Low-Speed Static Stability and Control Characteristics of a Model of a Right Triangular Pyramid Reentry Configuration. NASA MEMO 4-11-59L, 1959.

12. Mayo, Edward E.: Static Longitudinal Stability Characteristics of a Blunted Glider Reentry Configuration Having 79.5° Sweepback and 45° Dihedral at a Mach Number of 6.2 and Angles of Attack up to 20°. NASA TM X-222, 1959.

13. Whitcomb, Charles F., and Foss, Willard E., Jr.: Static Stability and Control Characteristics of Two Large-Dihedral Right Triangular Pyramid Lifting Reentry Configurations at a Mach Number of 3.05. NASA TM X-295, 1960.

14. Mugler, John P., Jr., and Olstad, Walter B.: Static Longitudinal Aerodynamic Characteristics at Transonic Speeds of a Blunted Right Triangular Pyramidal Lifting Reentry Configuration for Angles of Attack up to 110°. NASA TN D-797, 1961.

15. Spencer, Bernard, Jr.: Longitudinal Aerodynamic Characteristics at Mach Numbers From 0.40 to 1.10 of a Blunted Right Triangular Pyramidal Lifting Reentry Configuration Employing Variable-Sweep Wing Panels. NASA TN D-1518, 1963.

16. National Advisory Committee for Aeronautics: Aerodynamic Characteristics of Airfoils. NACA Rep. 315, 1929.

17. Braslow, Albert L., and Knox, Eugene C.: Simplified Method for Determination of Critical Height of Distributed Roughness Particles for Boundary-Layer Transition at Mach Numbers From 0 to 5. NACA TN 4363, 1958.

18. Cahn, Maurice S.: An Experimental Investigation of Sting-Support Effects on Drag and a Comparison With Jet Effects at Transonic Speeds. NACA Rep. 1353, 1958. (Supersedes NACA RM L56F18a.)

19. Polhamus, Edward C., Geller, Edward W., and Grunwald, Kalman J.: Pressure and Force Characteristics of Noncircular Cylinders as Affected by Reynolds Number With a Method Included for Determining the Potential Flow About Arbitrary Shapes. NASA TR R-46, 1959.

TABLE I.- FUSELAGE ORDINATES

x	y	z	
		Upper	Lower
0	0	0	0
1	.630	0	.630
2	.891	0	.891
4	1.261	0	1.261
6	1.544	.380	1.544
8	1.783	.380	1.783
10	1.993	.370	1.993
12	2.184	.350	2.184
14	2.359	.280	2.359
16	2.522	0	2.522
18	2.675	0	2.640
20	2.819	0	2.670

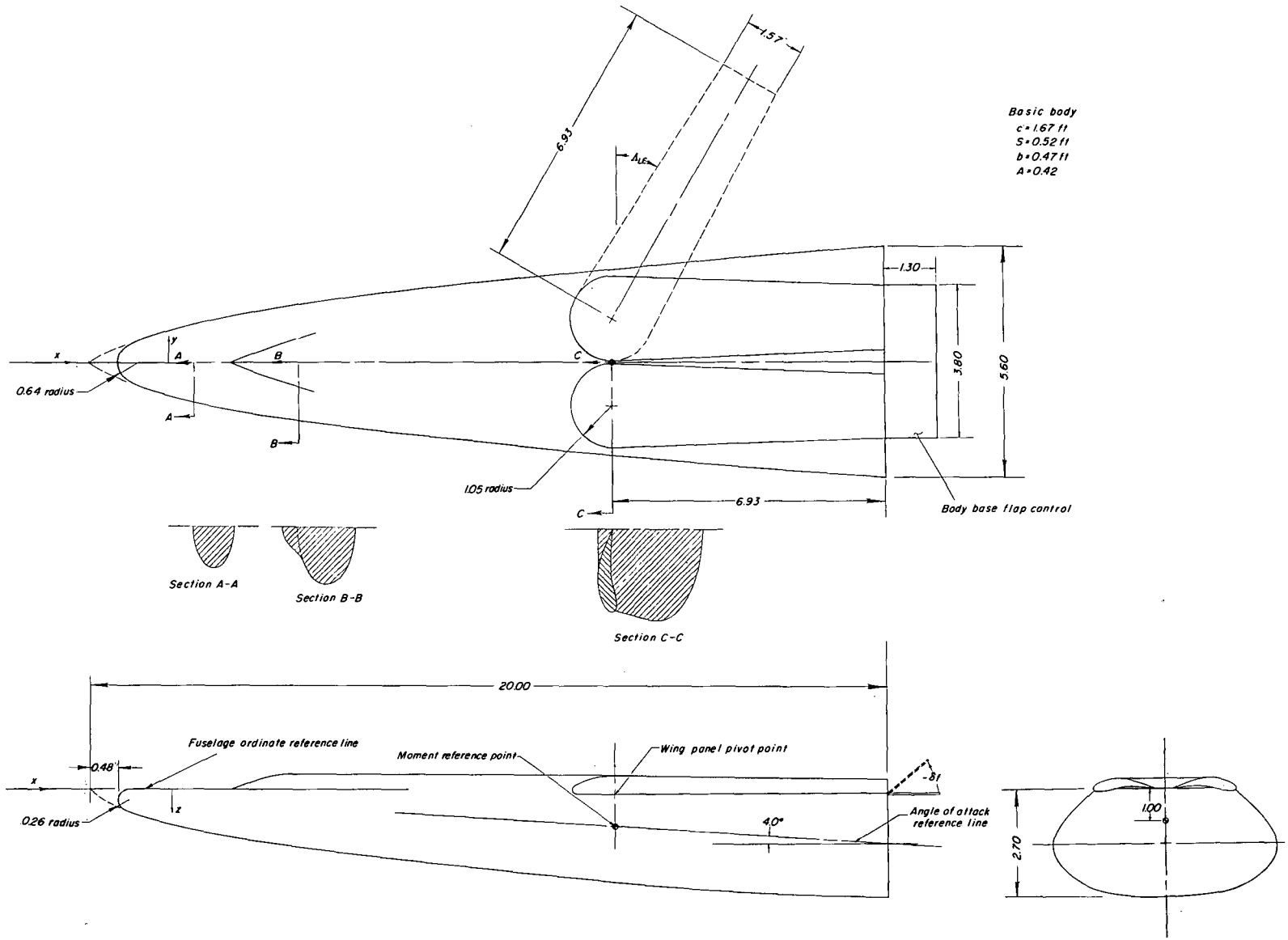

Figure 1.- Three-view drawing of model. All dimensions are in inches unless otherwise noted.

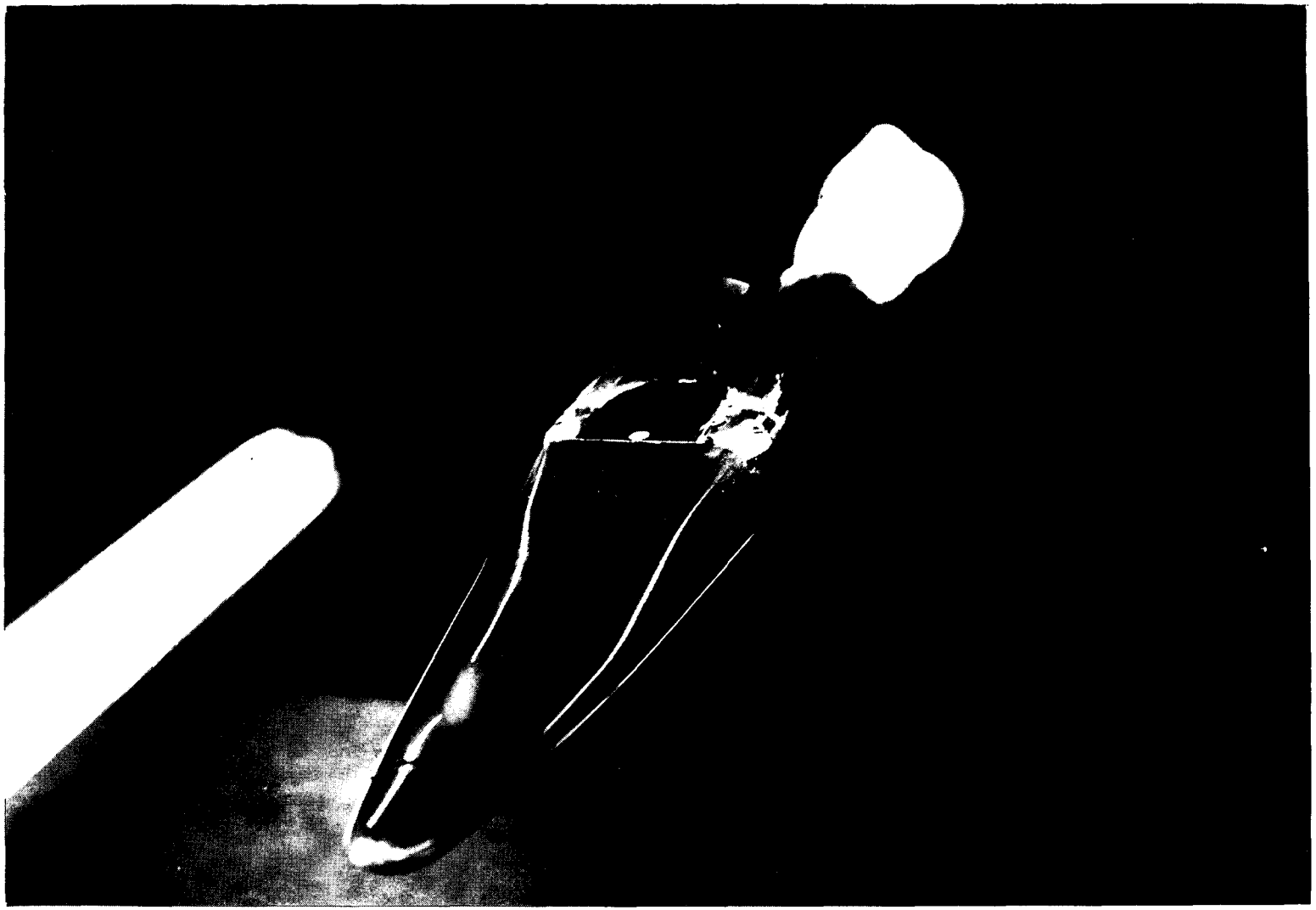

(a) Wing panels retracted. $\Lambda_{LE} = 90^{\circ}$. L-62-6104

Figure 2.- Photographs of configuration with wing panels in various positions; body-base flap off.

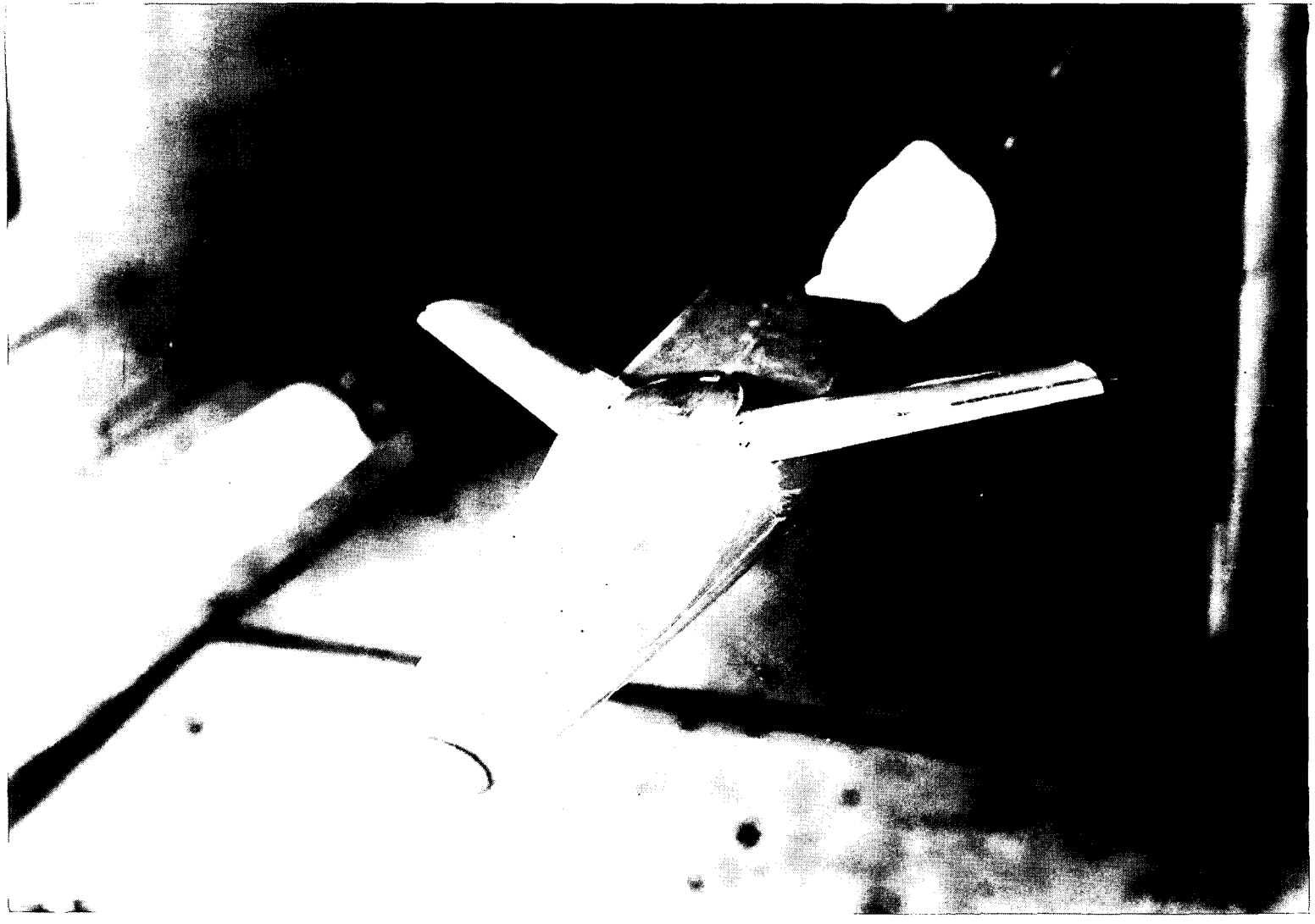

(b) Wing panels extended. $\Lambda_{LE} = 40^{\circ}$. L-62-6103

Figure 2.- Continued.

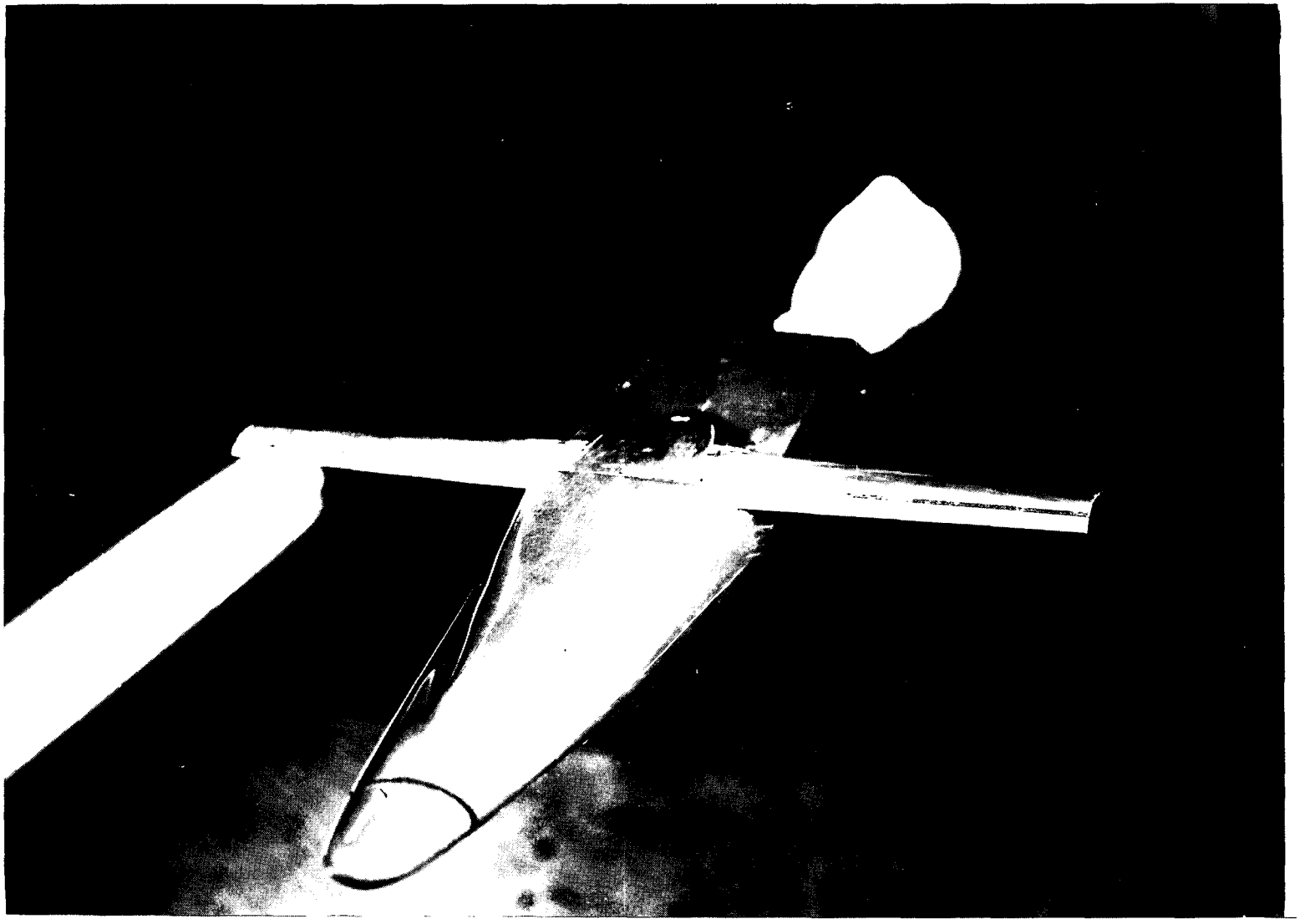

(c) Wing panels fully extended. $\Lambda_{LE} = 0^{\circ}$. L-62-6105

Figure 2.- Concluded.

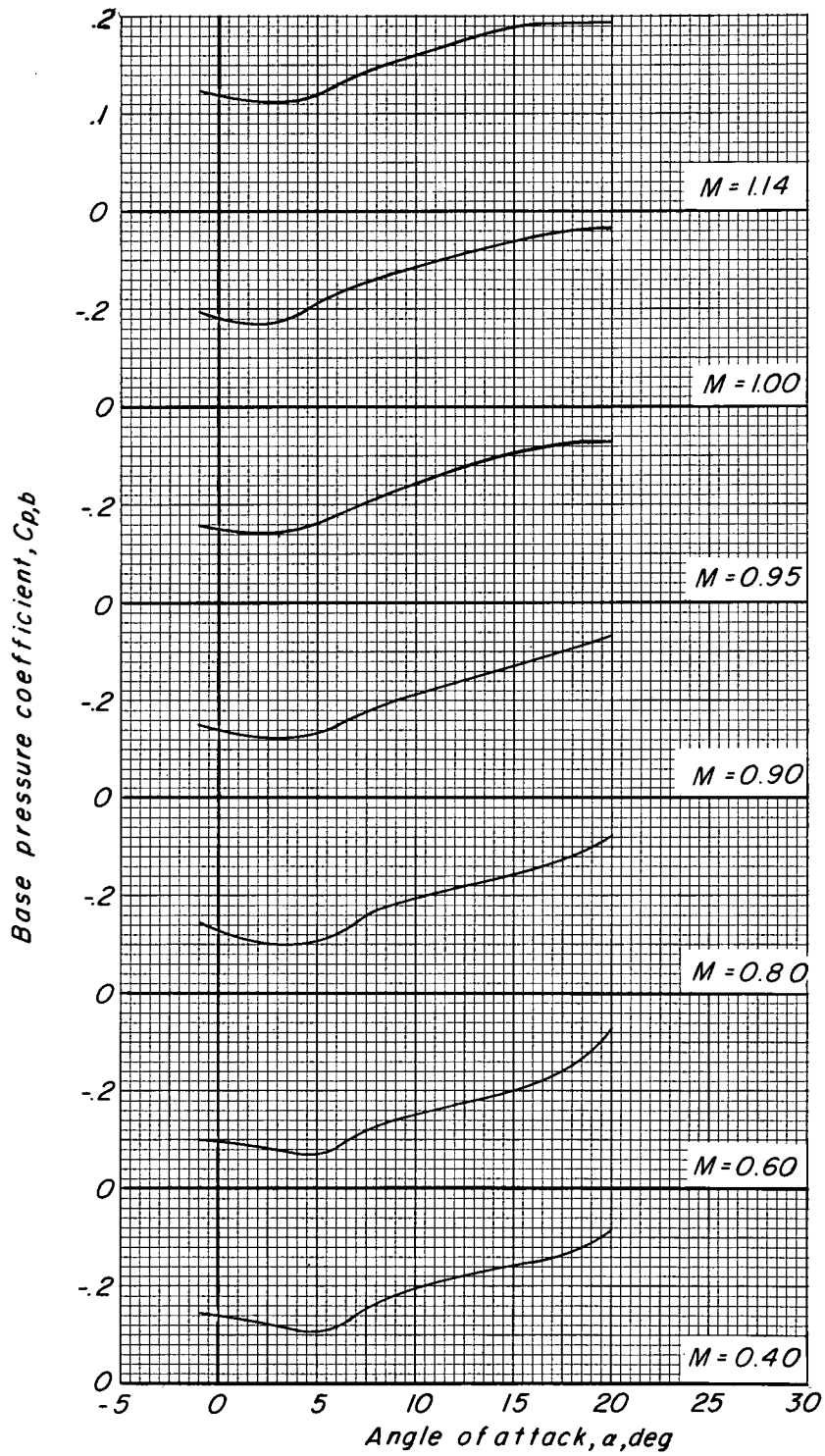

Figure 3.- Variation of base pressure coefficient with increasing angle of attack and various Mach numbers for basic configuration ($\Lambda_{LE} = 90^{\circ}$); body-base flap off.

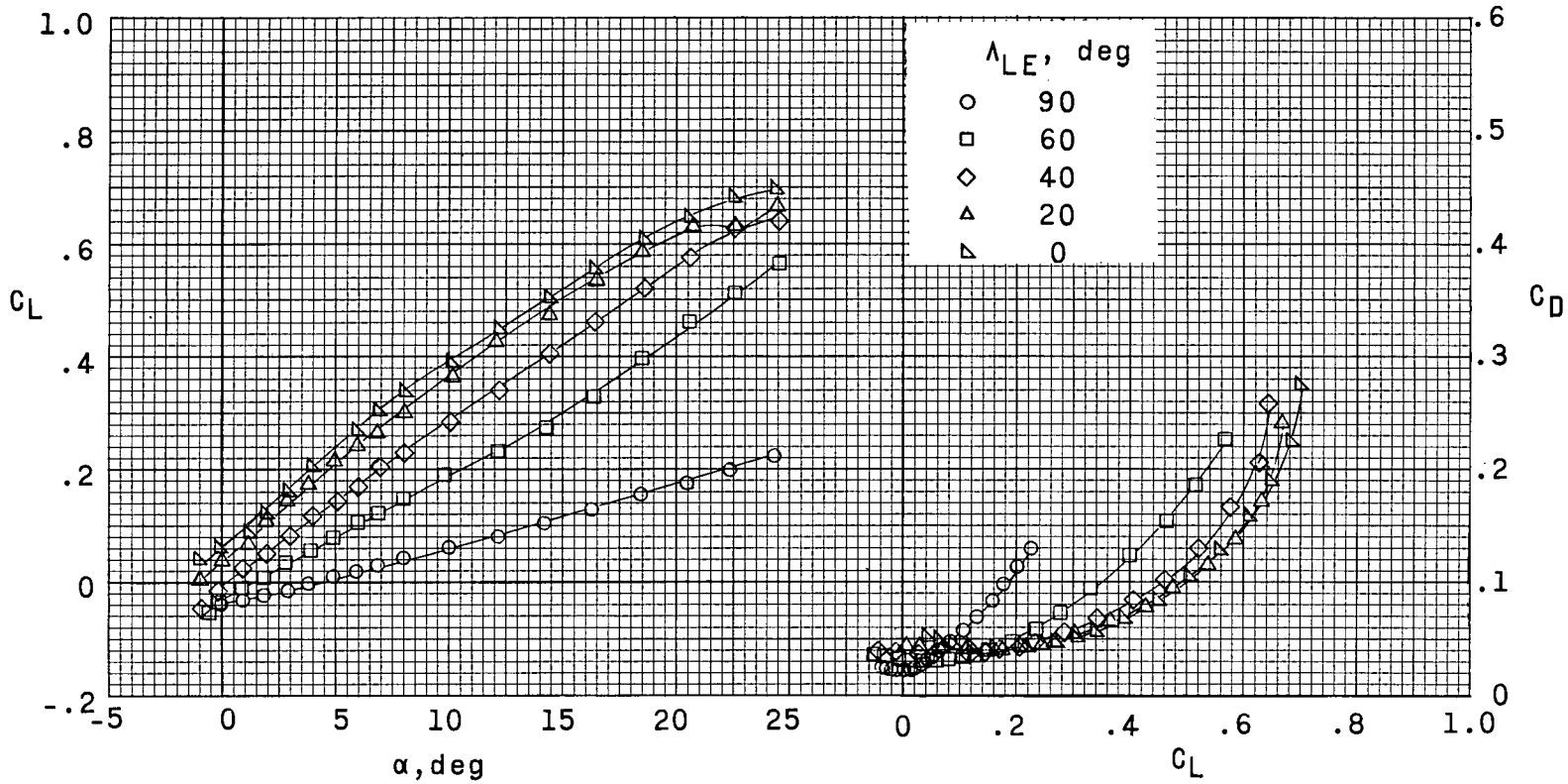

(a) M = 0.40.

Figure 4.- Effects of wing-panel sweep on longitudinal aerodynamic characteristics of basic configuration without body-base flap. (Solid symbols indicate variation of L/D with C_L.)

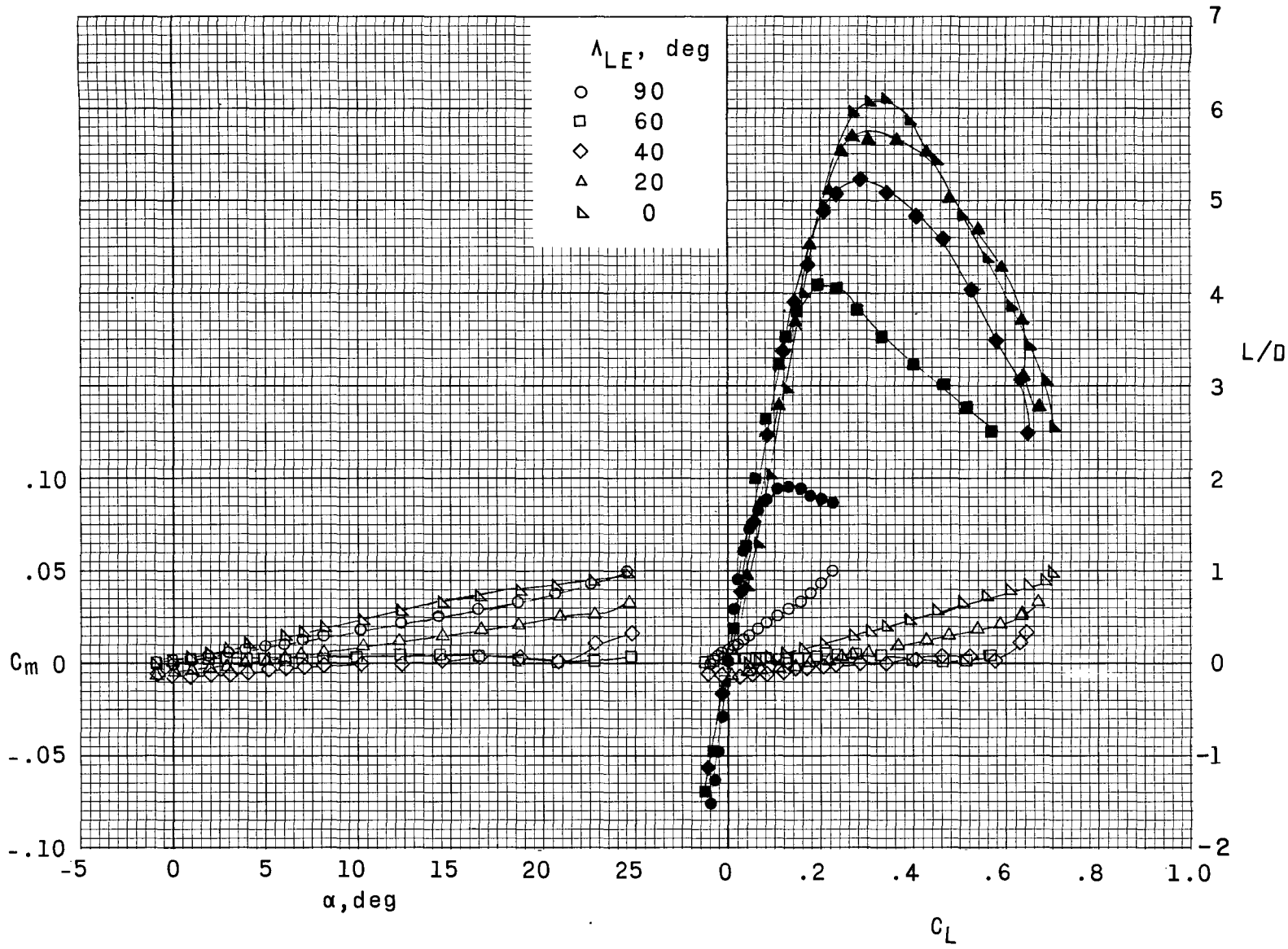

(a) Concluded.

Figure 4.- Continued.

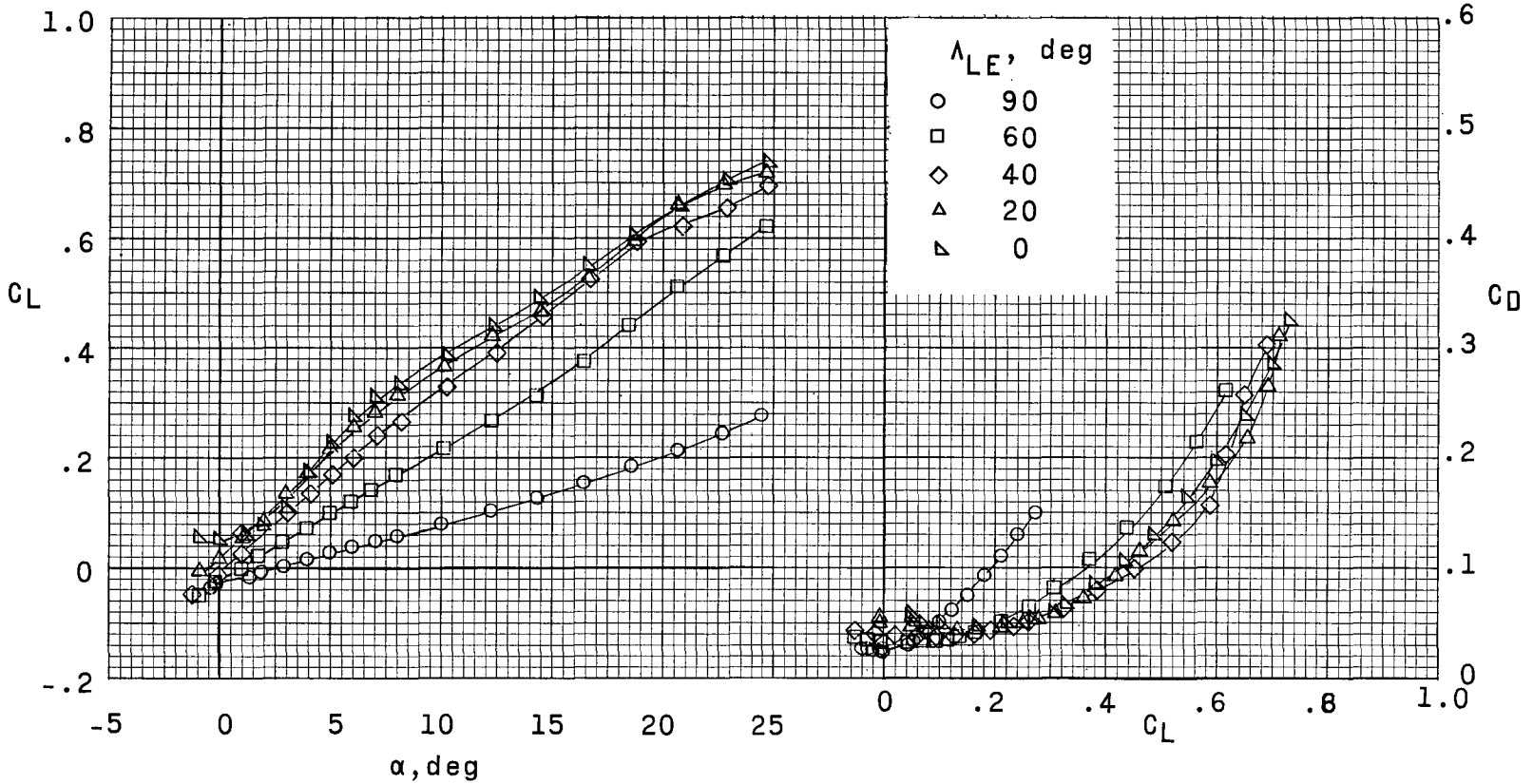

(b) M = 0.60.

Figure 4.- Continued.

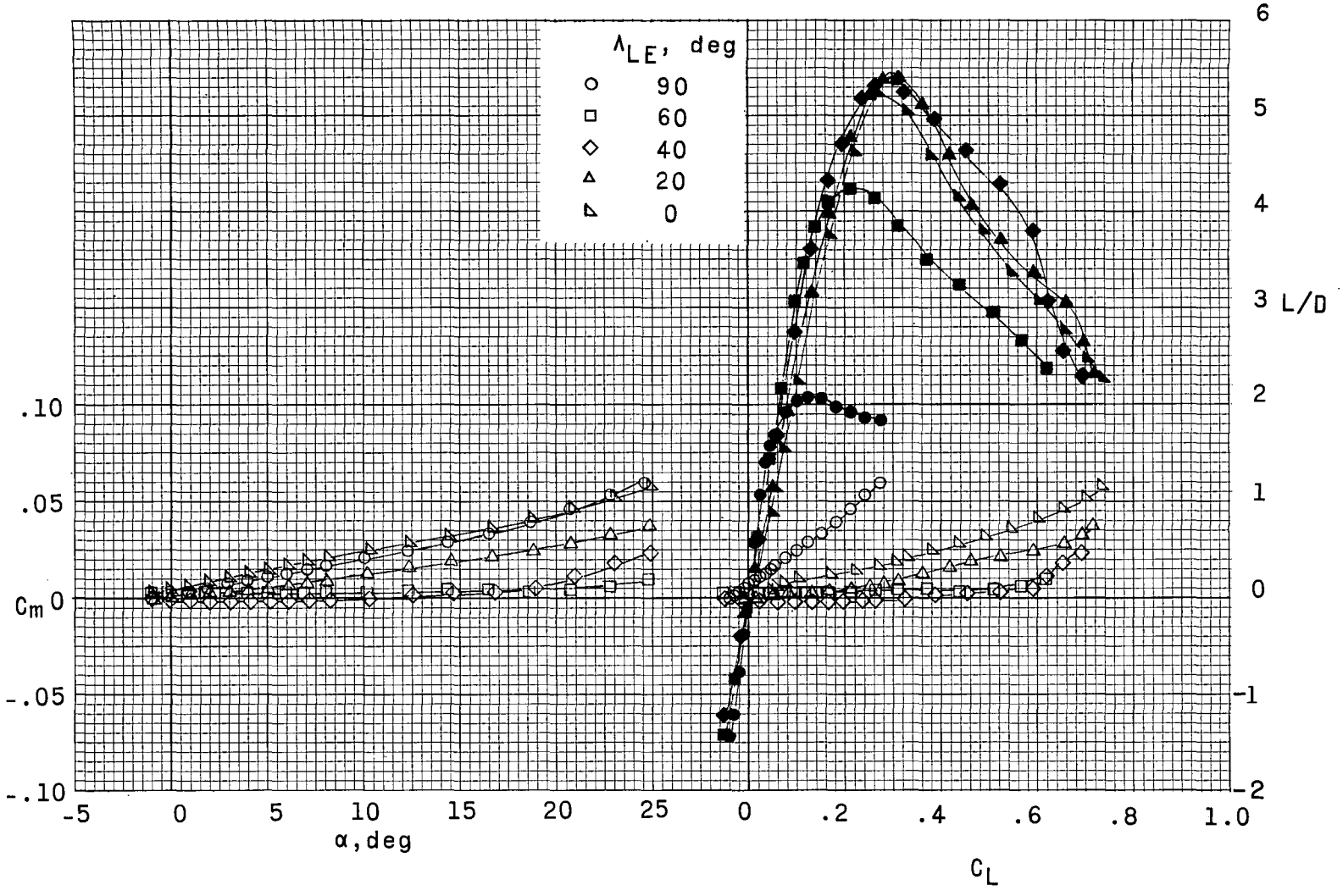

(b) Concluded.

Figure 4.- Continued.

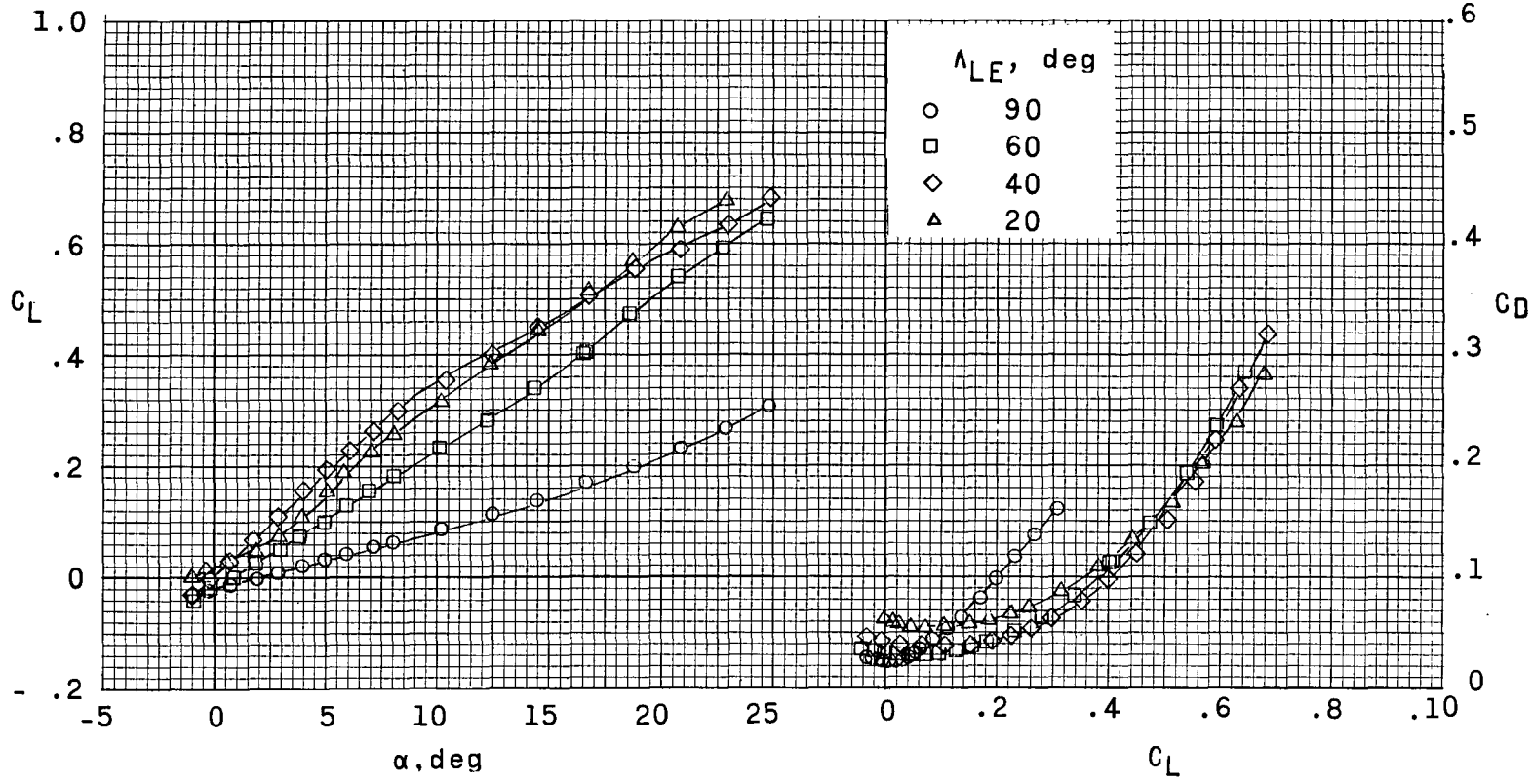

(c) M = 0.80.

Figure 4.- Continued.

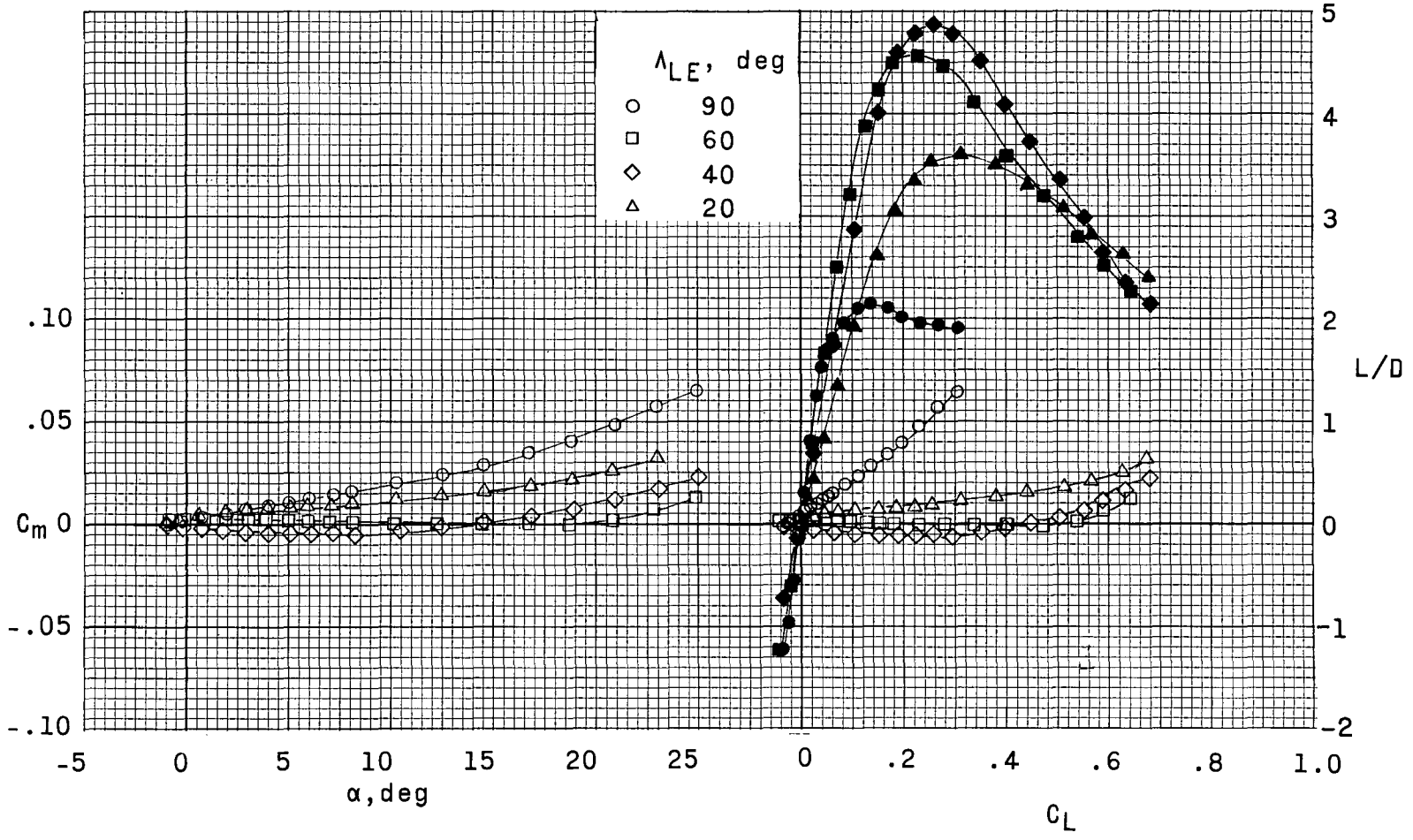

(c) Concluded.

Figure 4.- Continued.

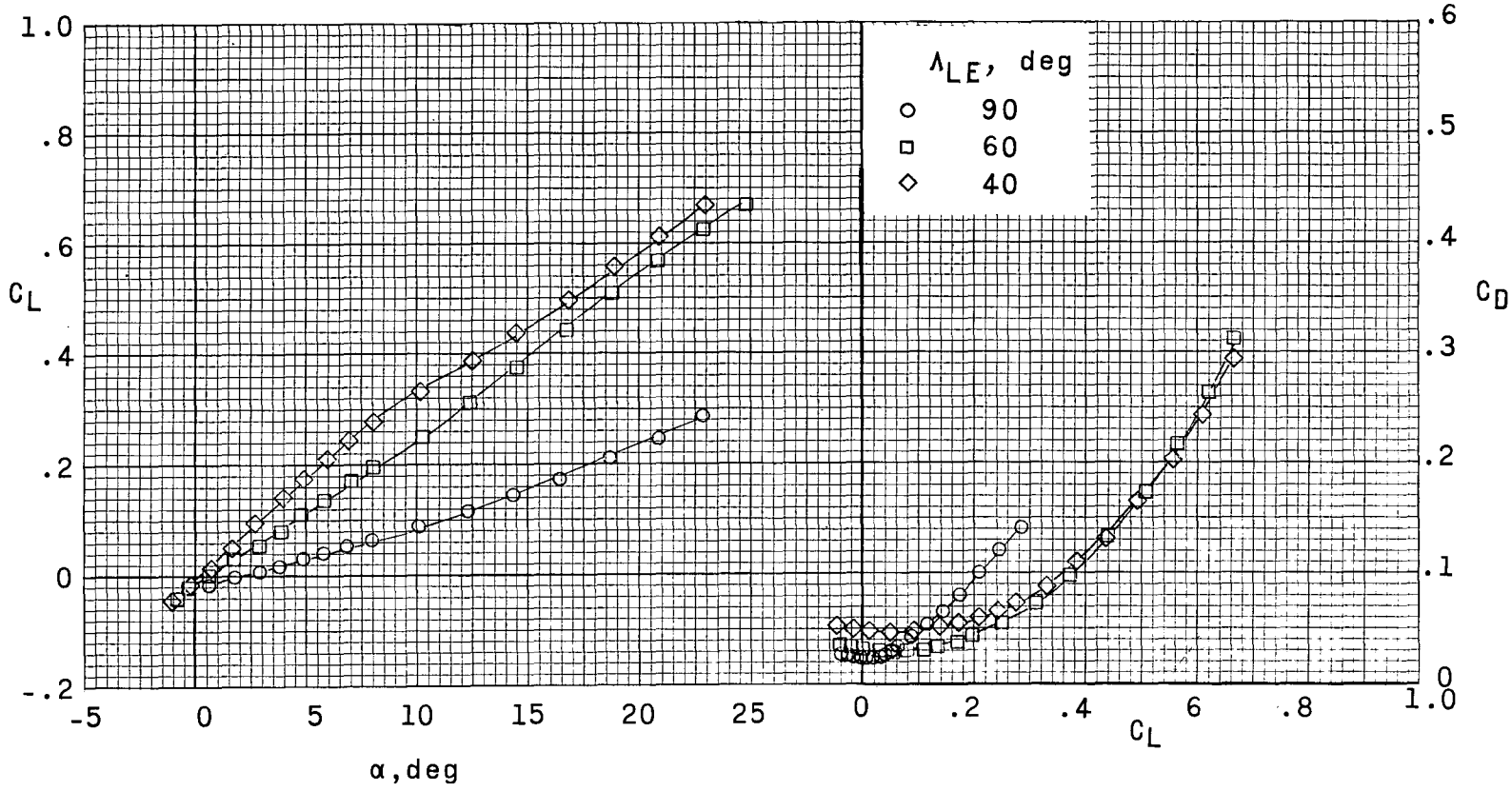

(d) M = 0.90.

Figure 4.- Continued.

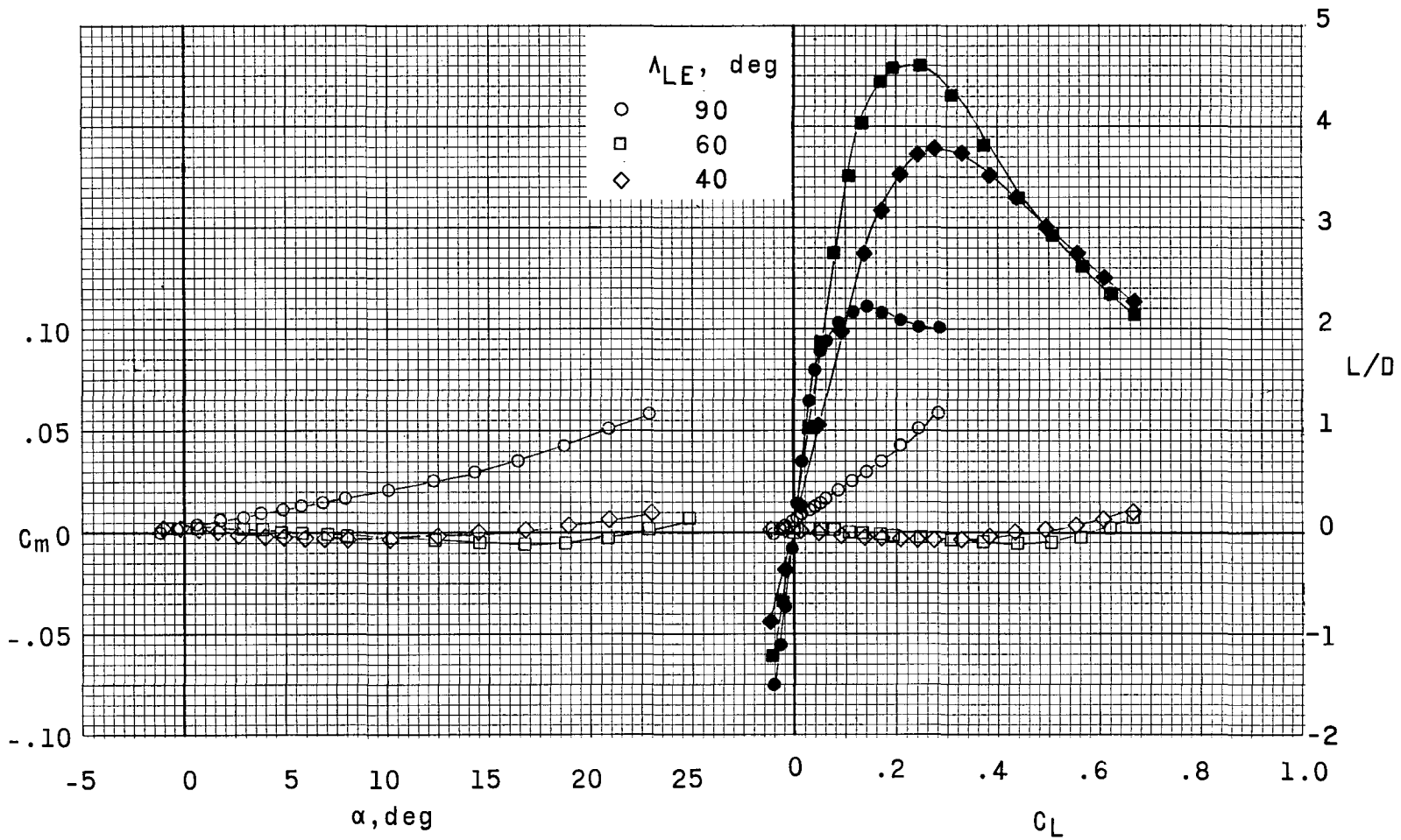

(d) Concluded.

Figure 4.- Continued.

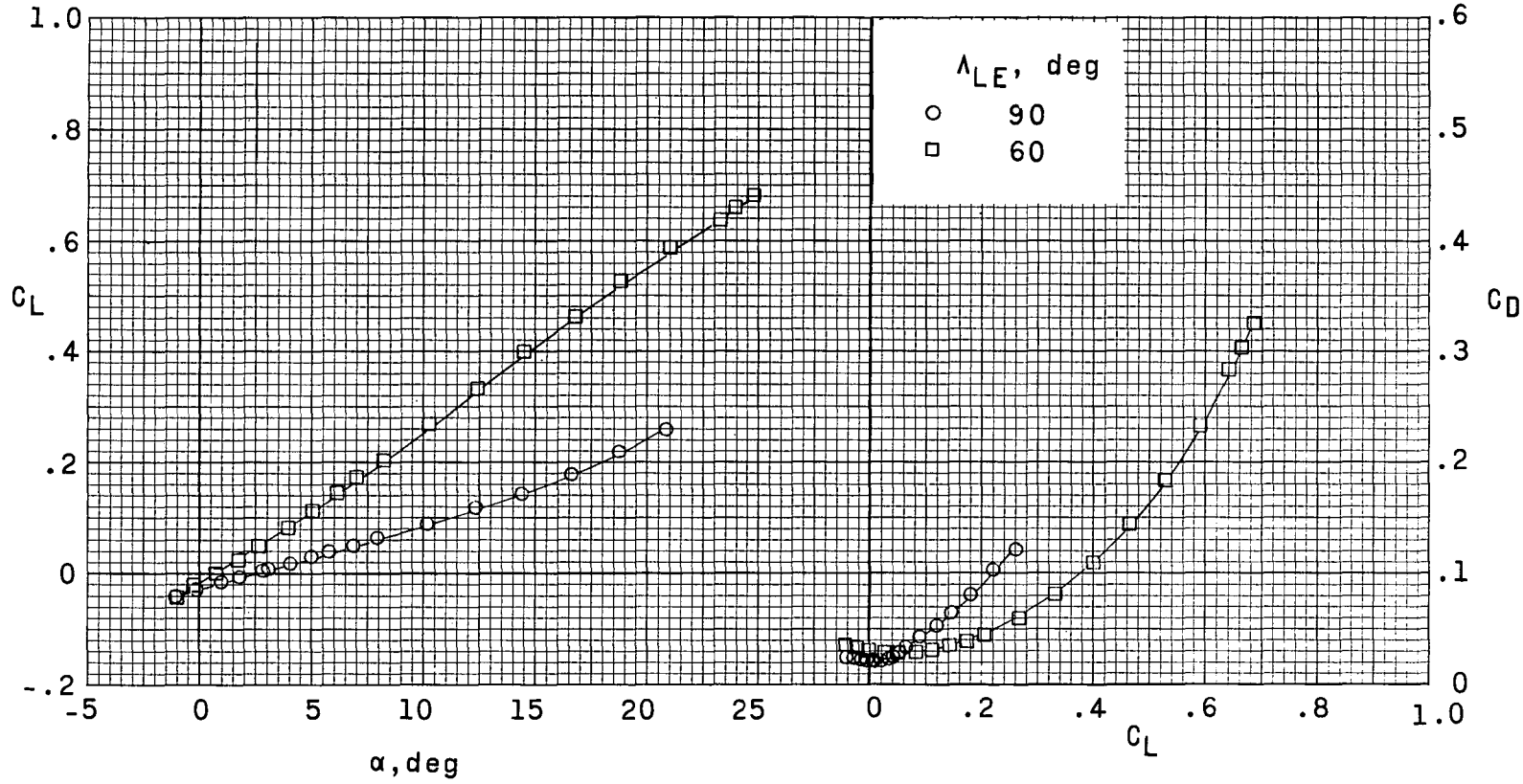

(e) M = 0.95.

Figure 4.- Continued.

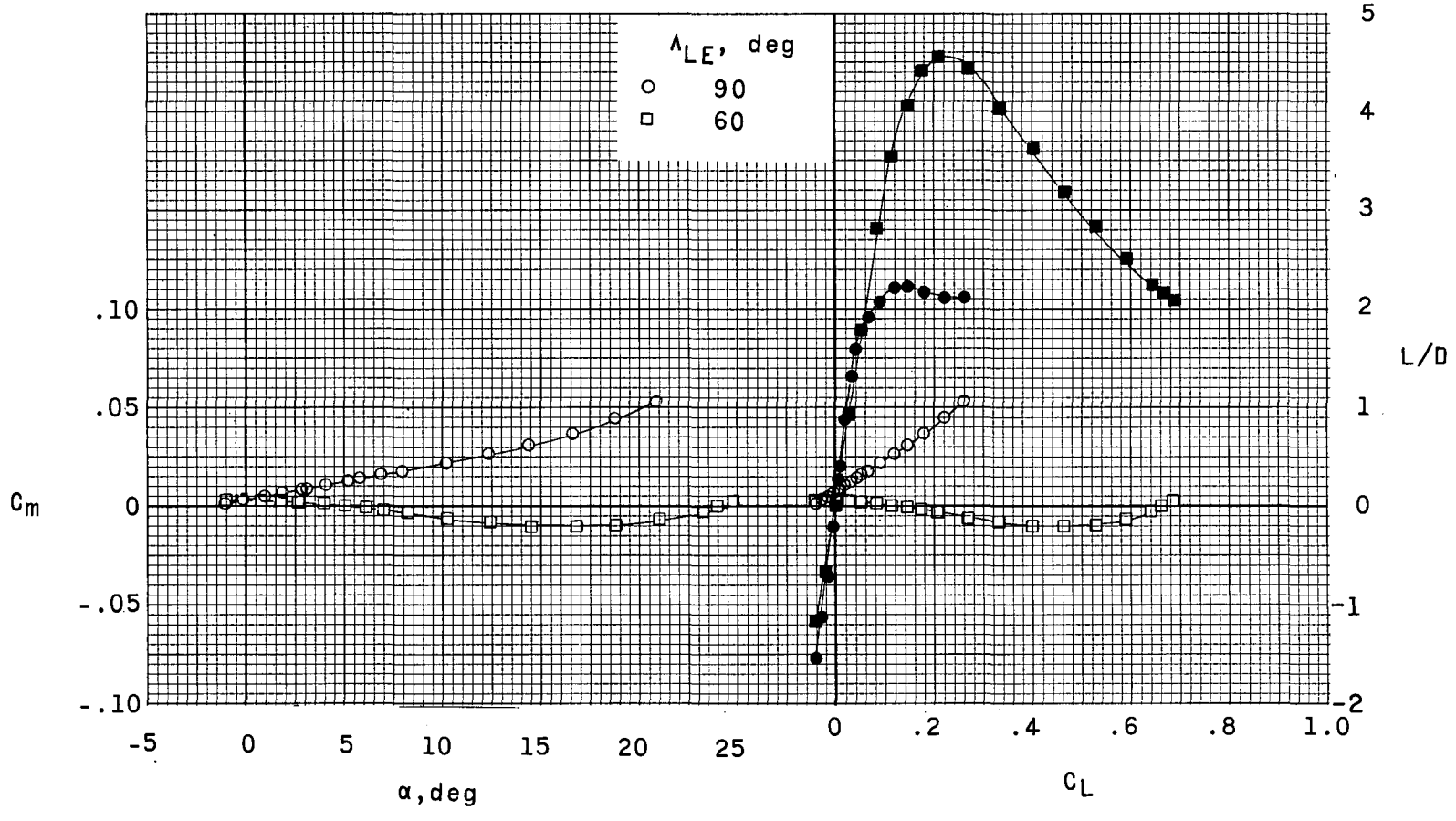

(e) Concluded.

Figure 4.- Continued.

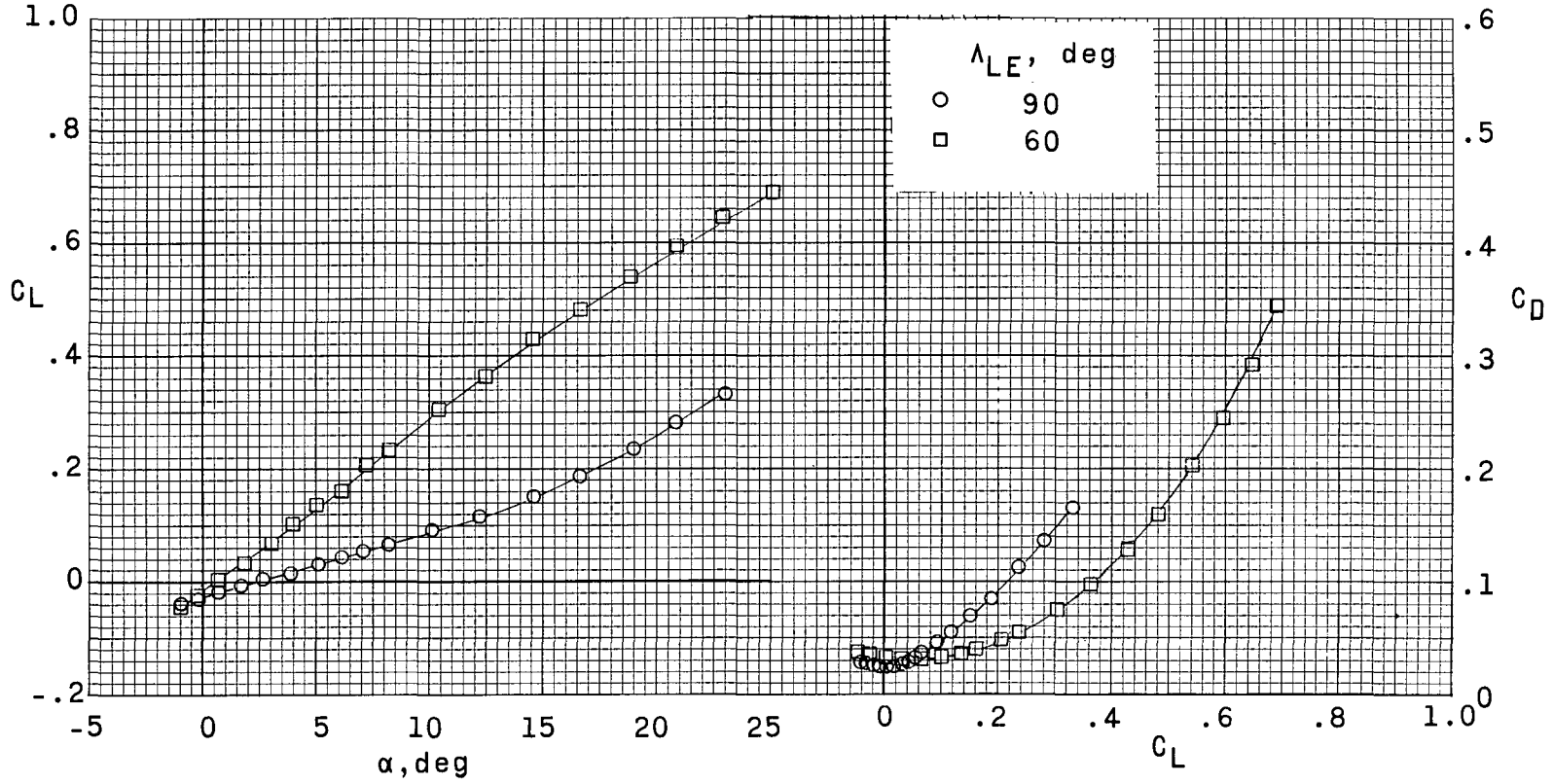

(f) M = 1.00.

Figure 4.- Continued.

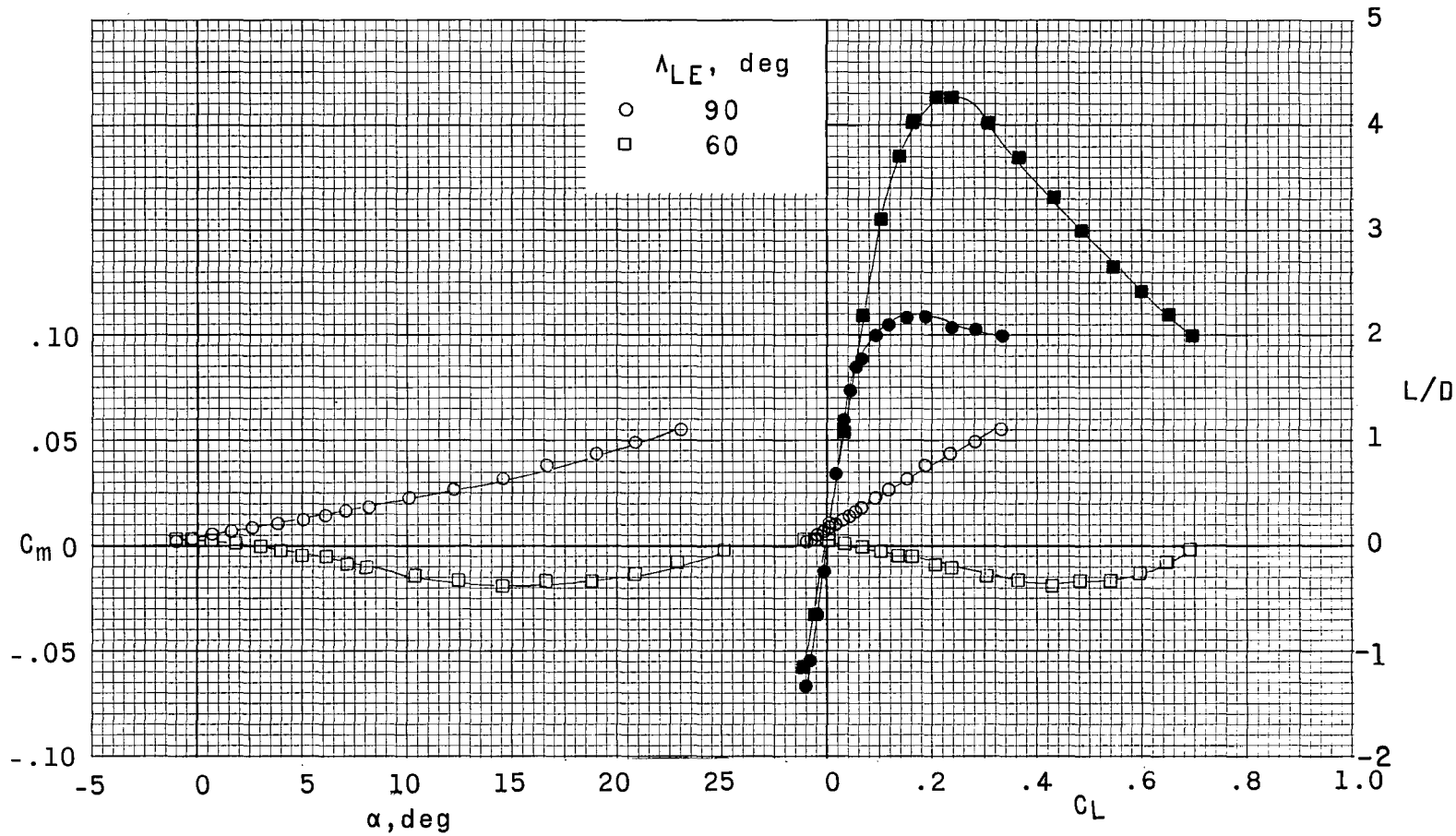

(f) Concluded.

Figure 4.- Continued.

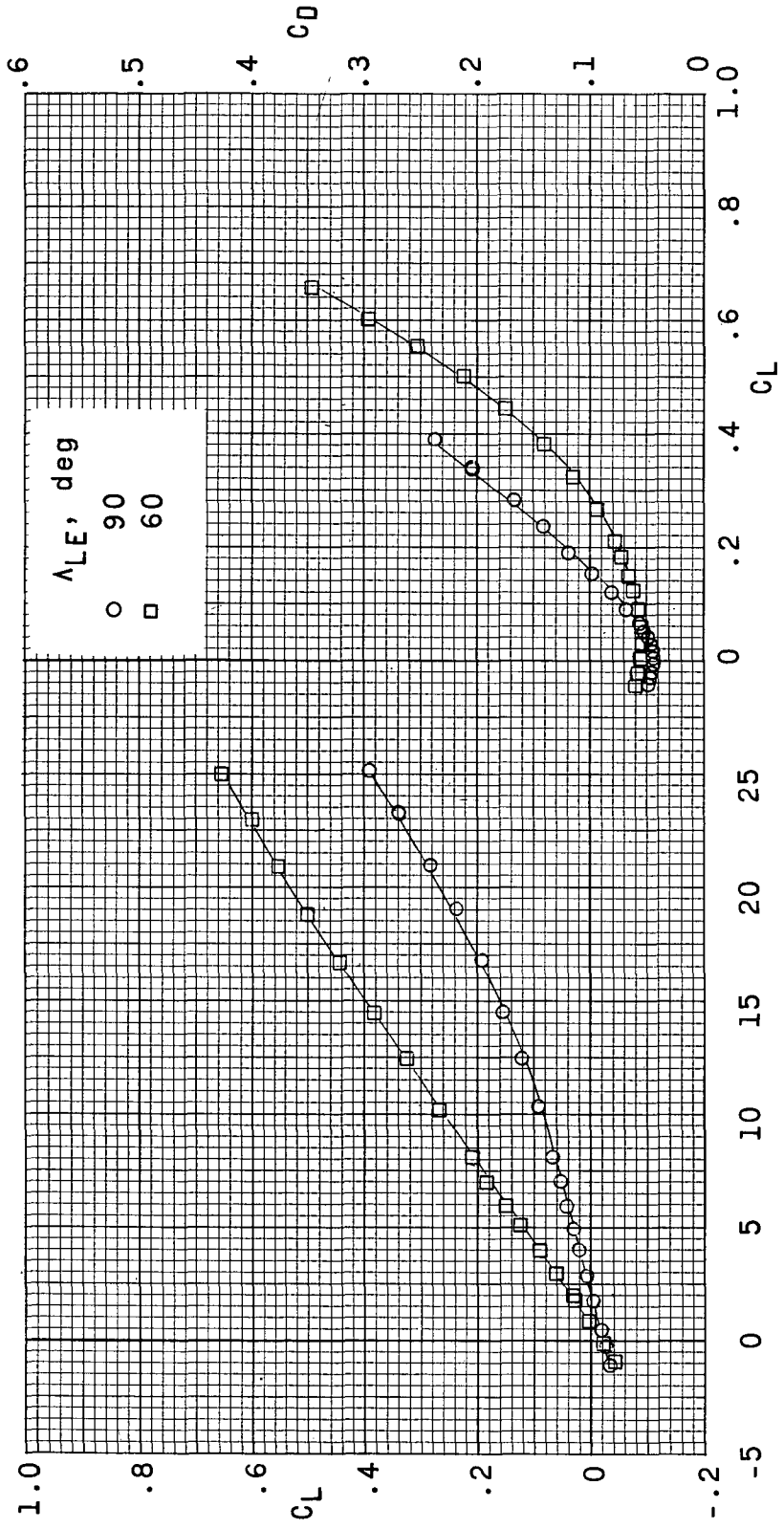

(g) M = 1.14.

Figure 4.- Continued.

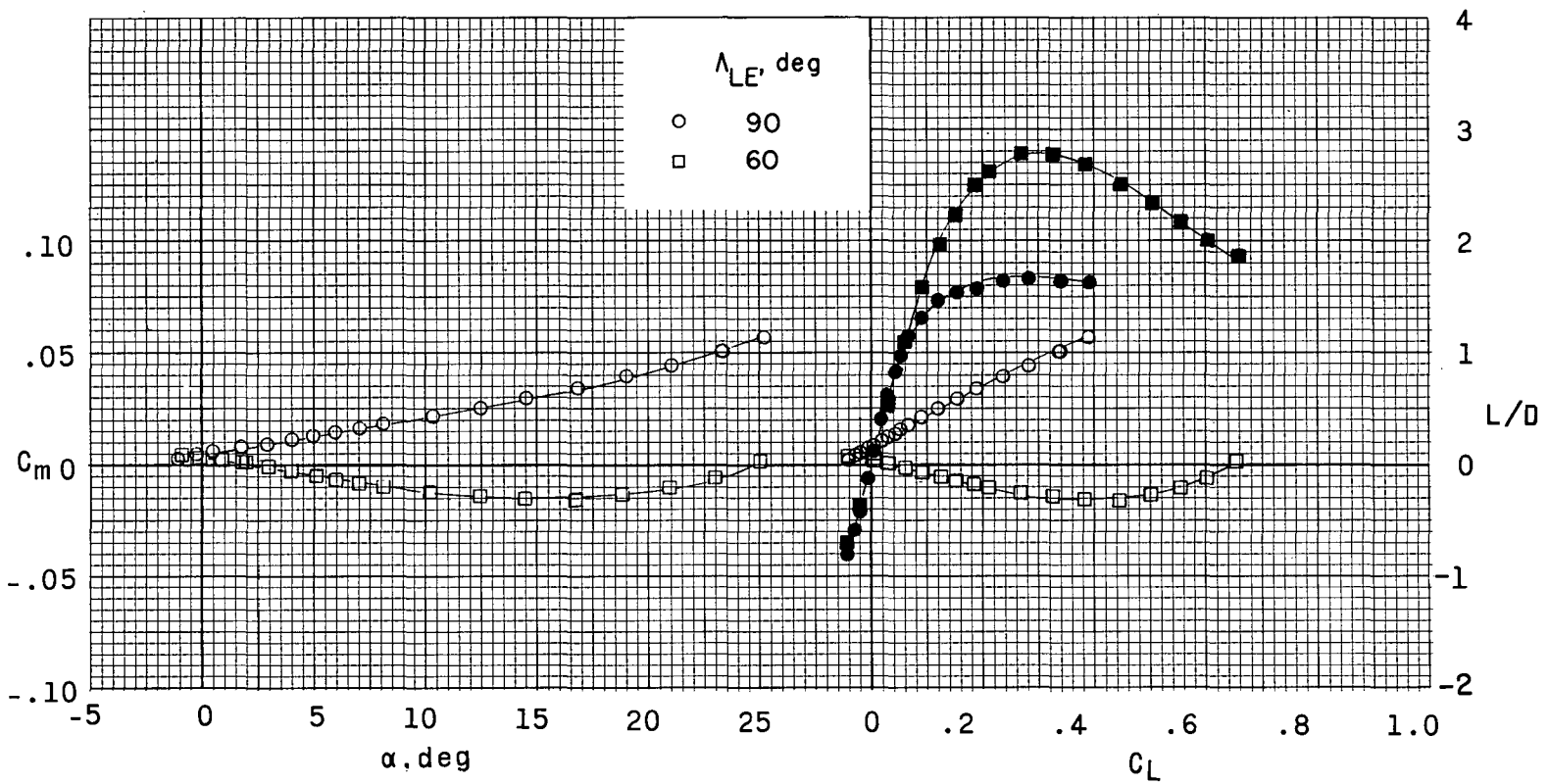

(g) Concluded.

Figure 4.- Concluded.

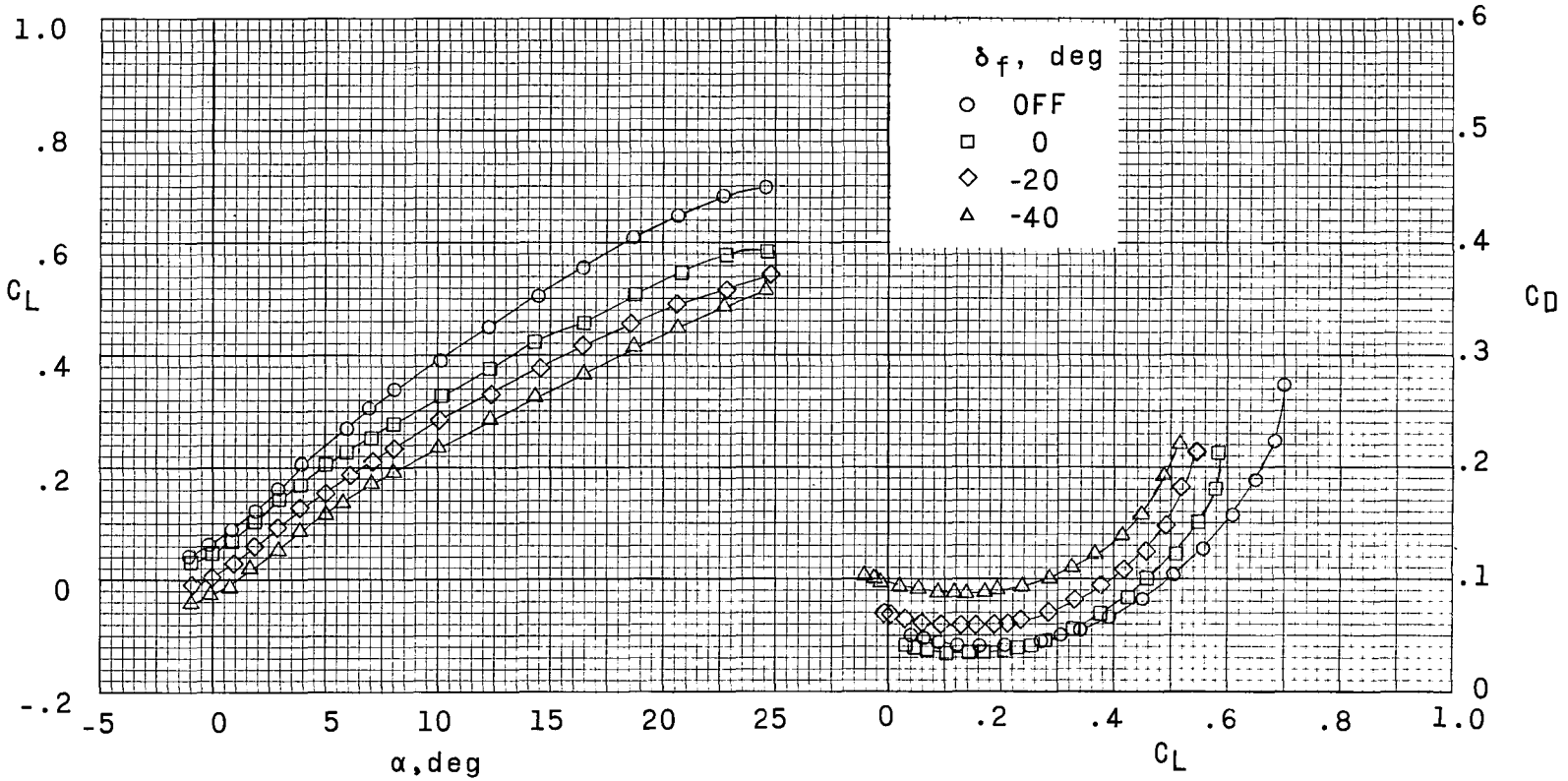

(a) $\Lambda_{LE} = 0^{\circ}$.

Figure 5.- Effects of addition and deflection of a body-base flap control on longitudinal aerodynamic characteristics of configuration with various wing-panel sweeps. M = 0.40. (Solid symbols indicate variations of L/D with C_L.)

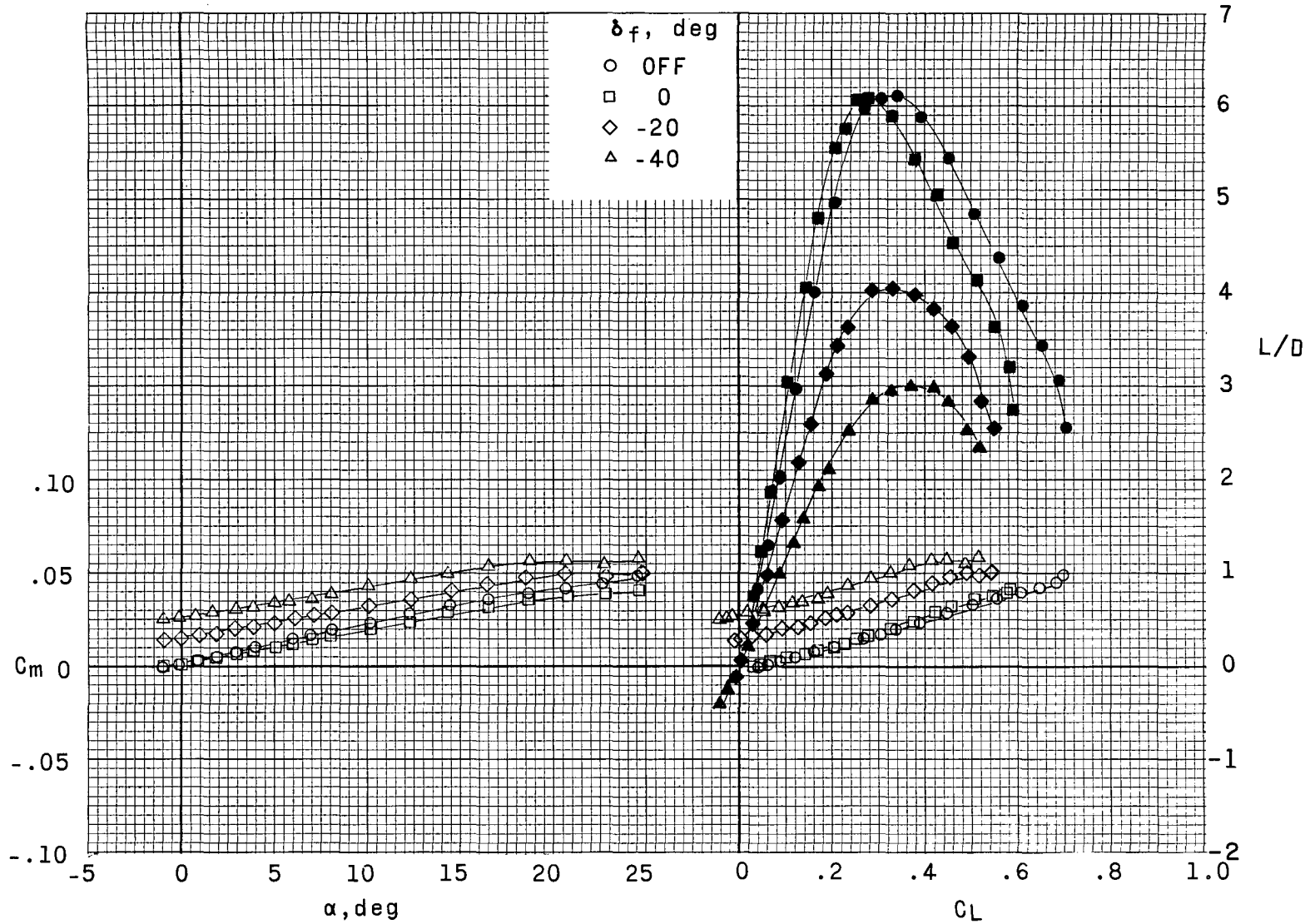

(a) Concluded.

Figure 5.- Continued.

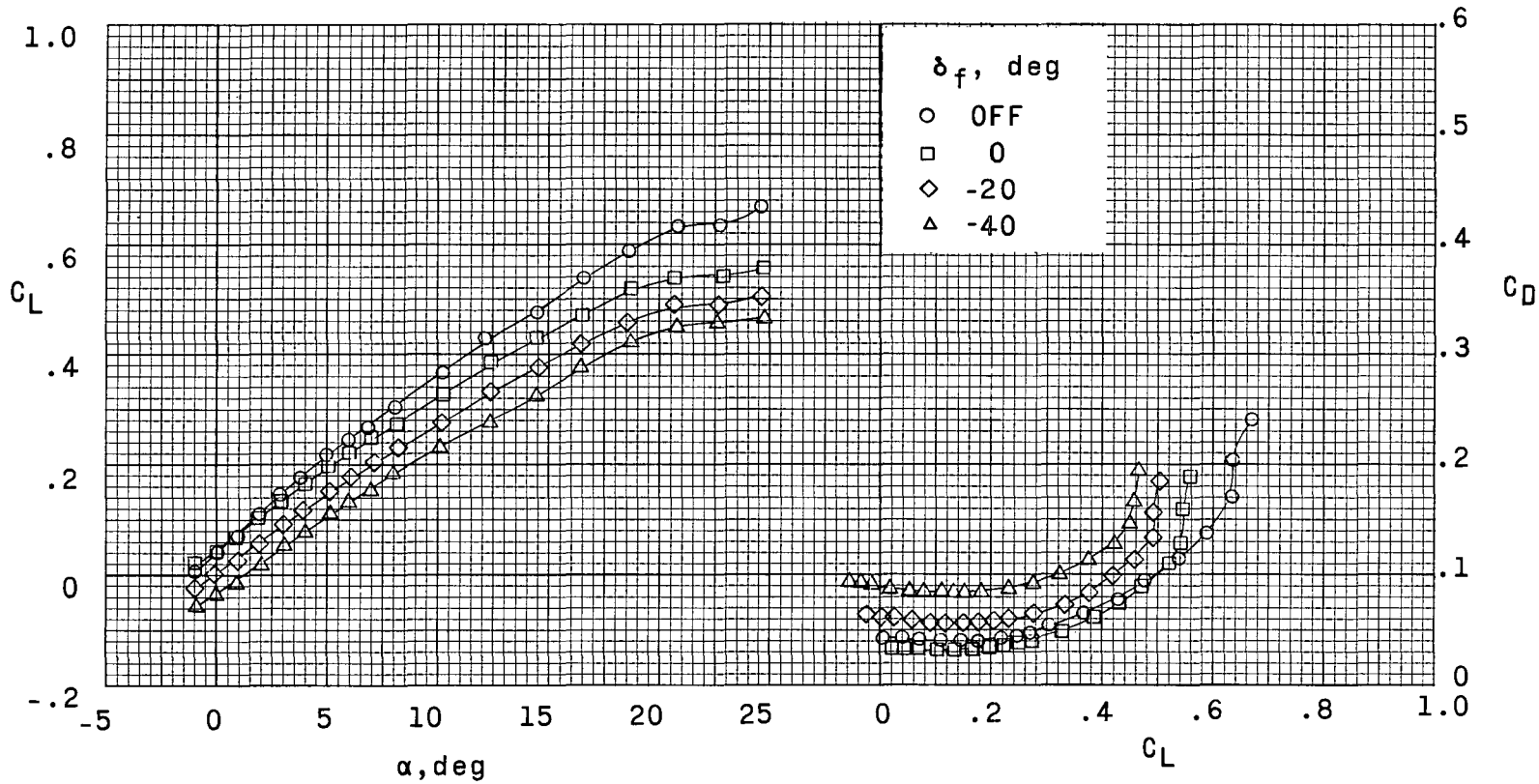

(b) $\Lambda_{LE} = 20^\circ$.

Figure 5.- Continued.

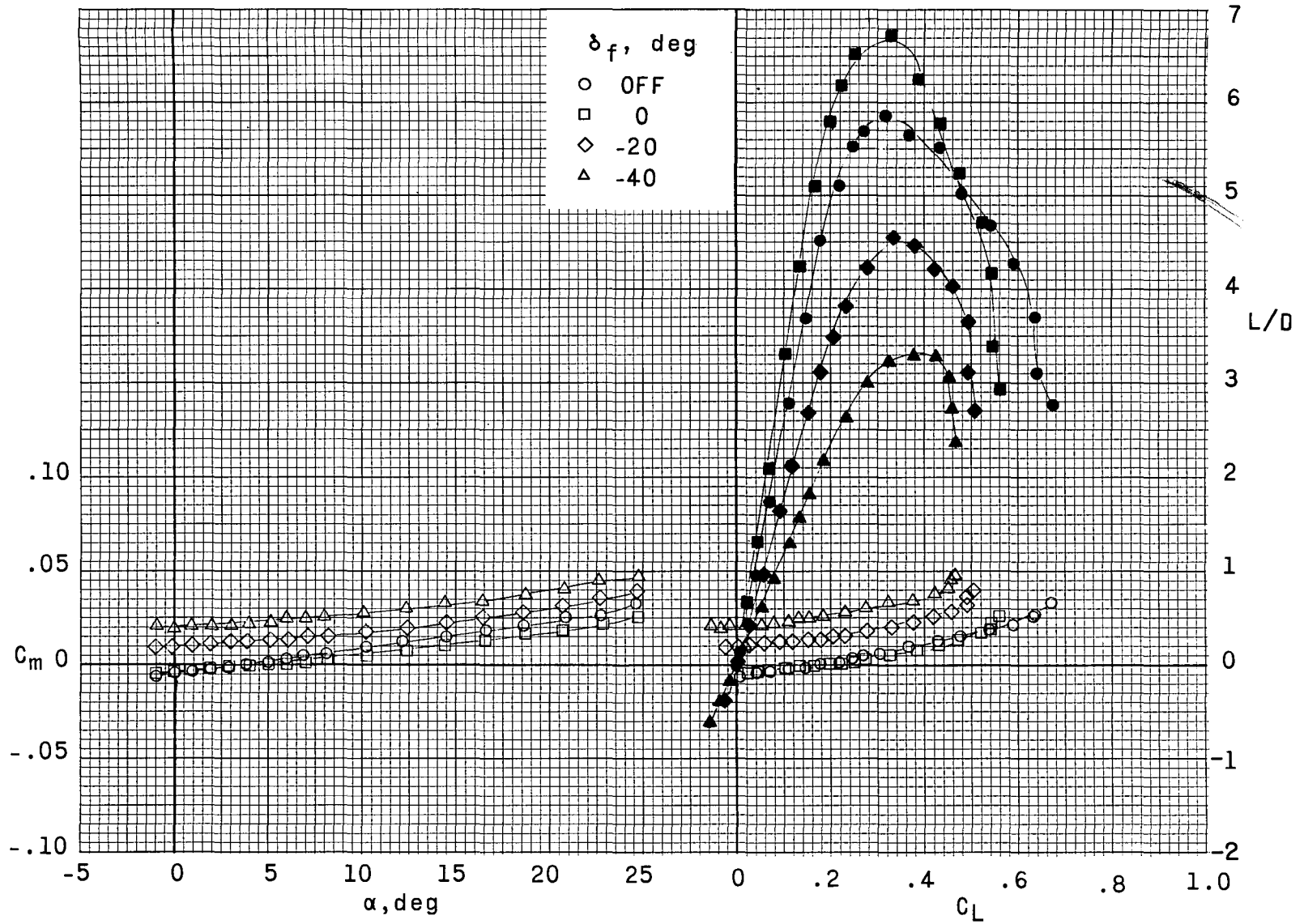

(b) Concluded.

Figure 5.- Continued.

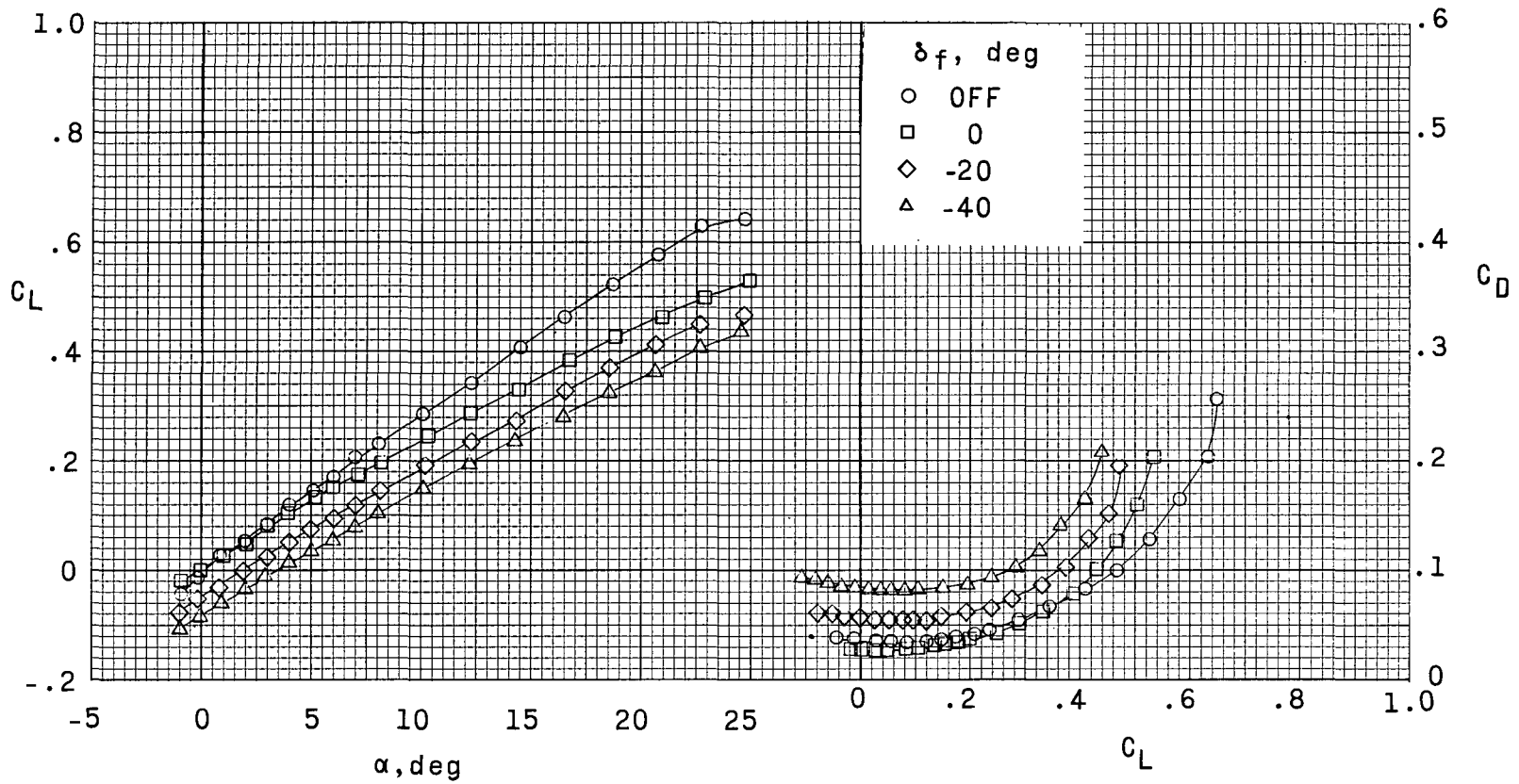

(c) $\Lambda_{LE} = 40°$.

Figure 5.- Continued.

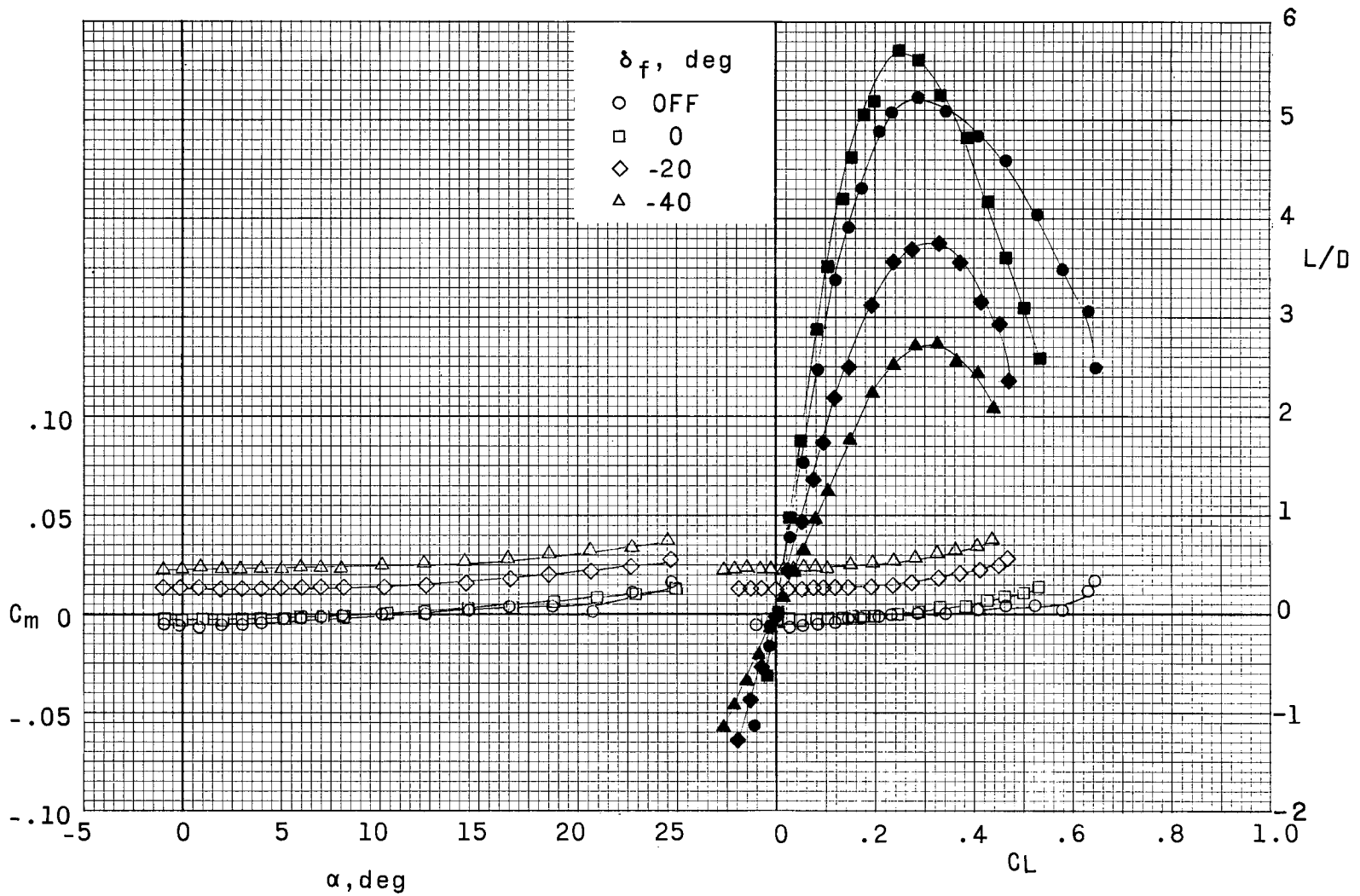

(c) Concluded.

Figure 5.- Continued.

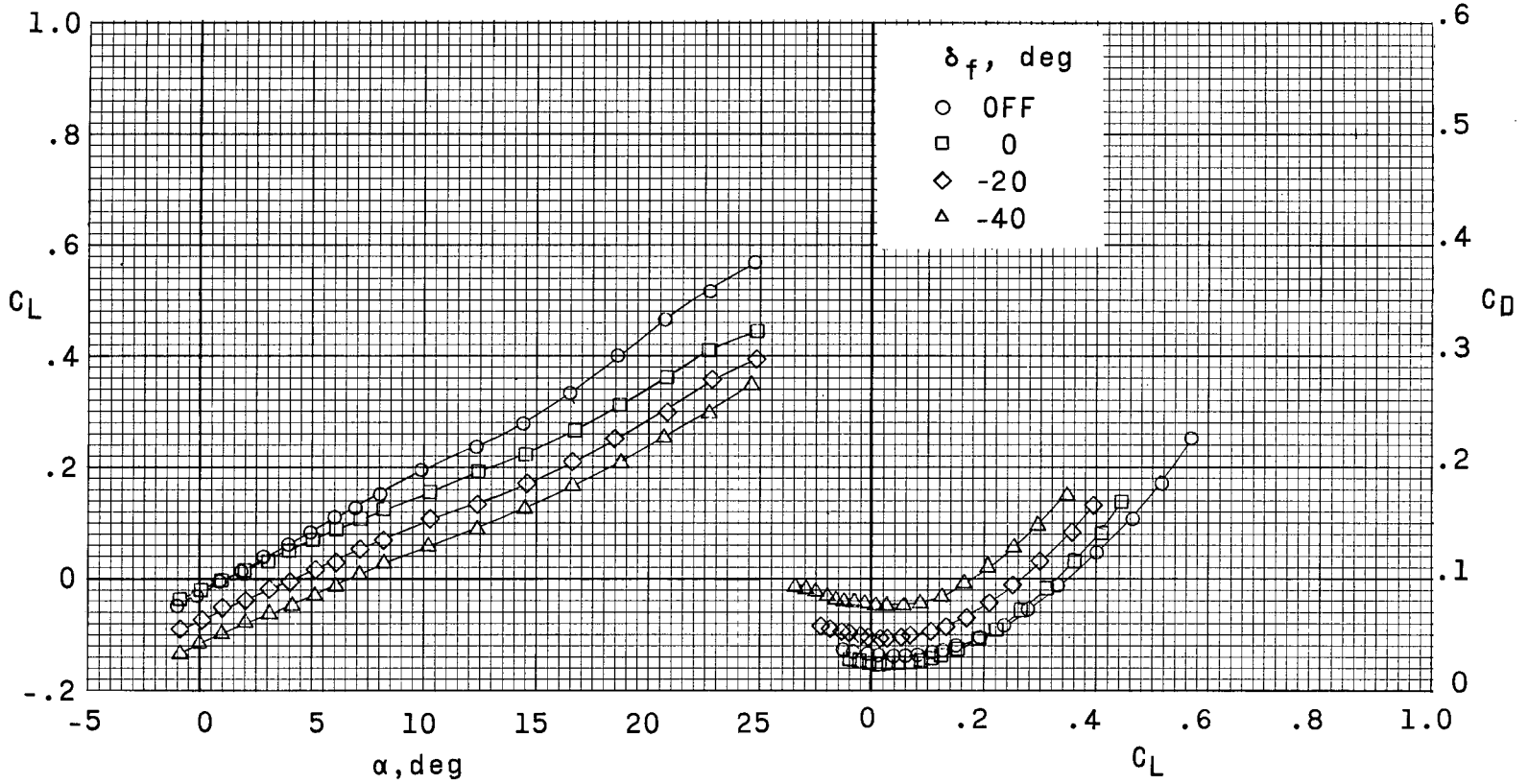

(d) $\Lambda_{LE} = 60°$.

Figure 5.- Continued.

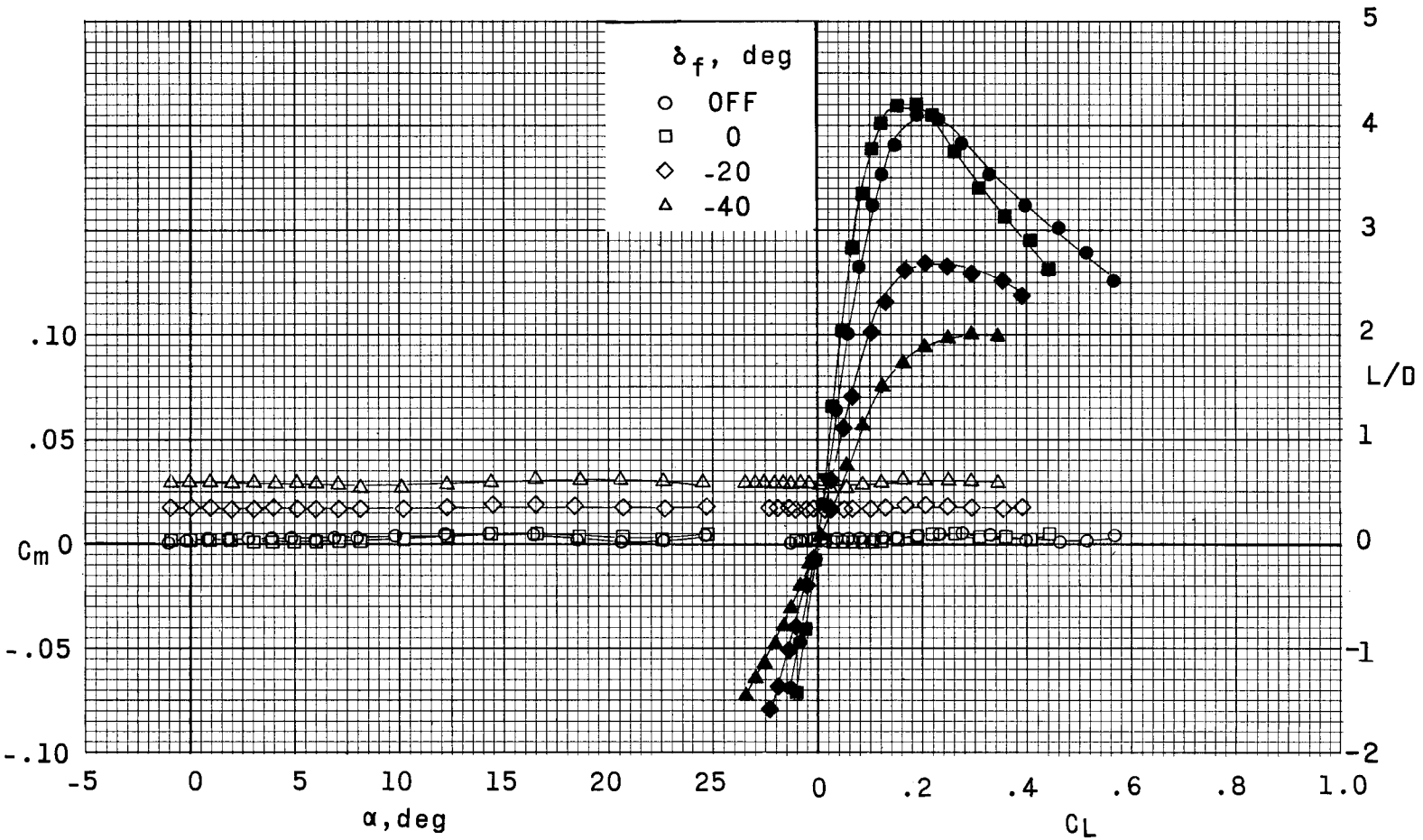

(d) Concluded.

Figure 5.- Continued.

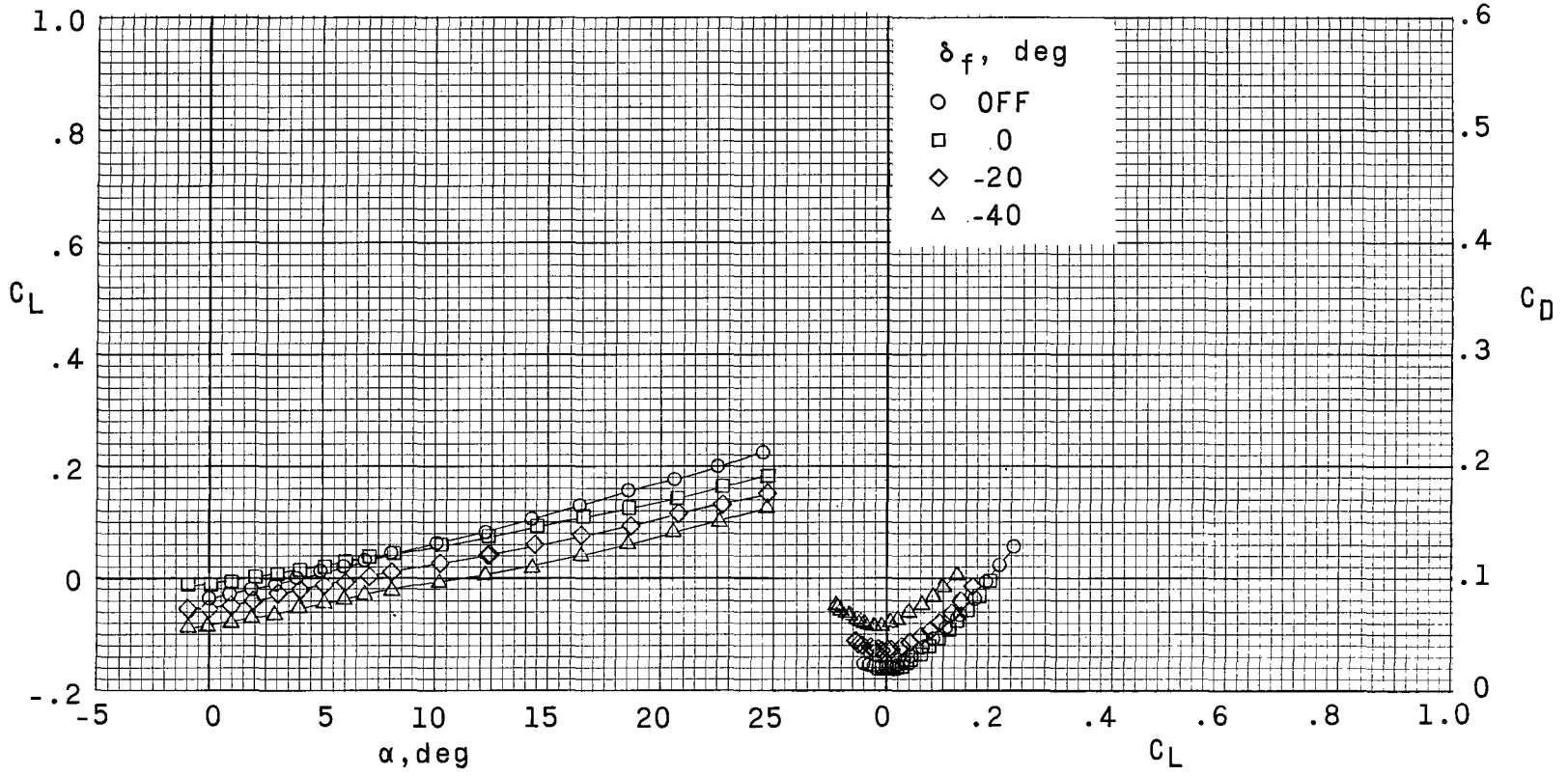

(e) $\Lambda_{LE} = 90^{\circ}$.

Figure 5.- Continued.

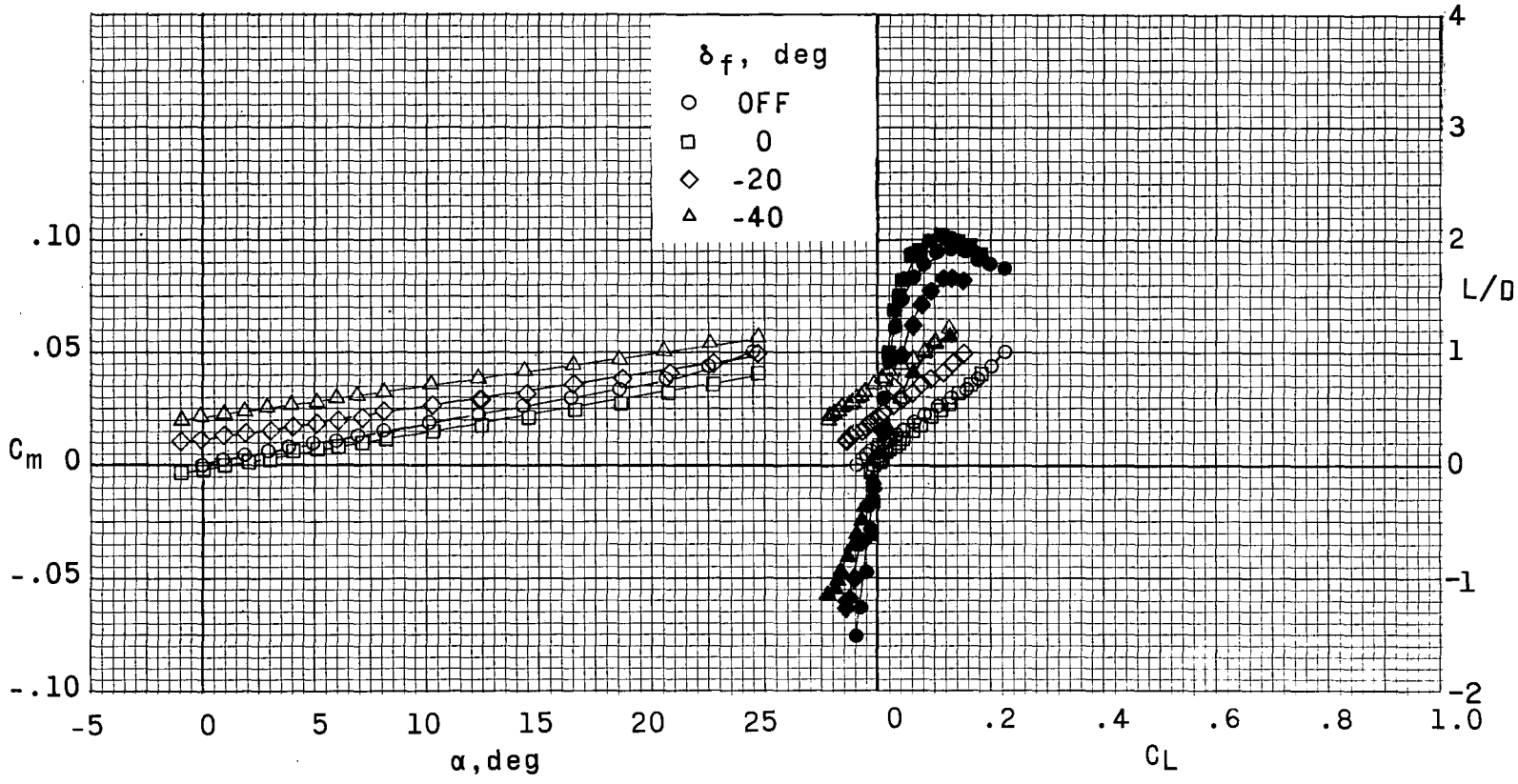

(e) Concluded.

Figure 5.- Concluded.

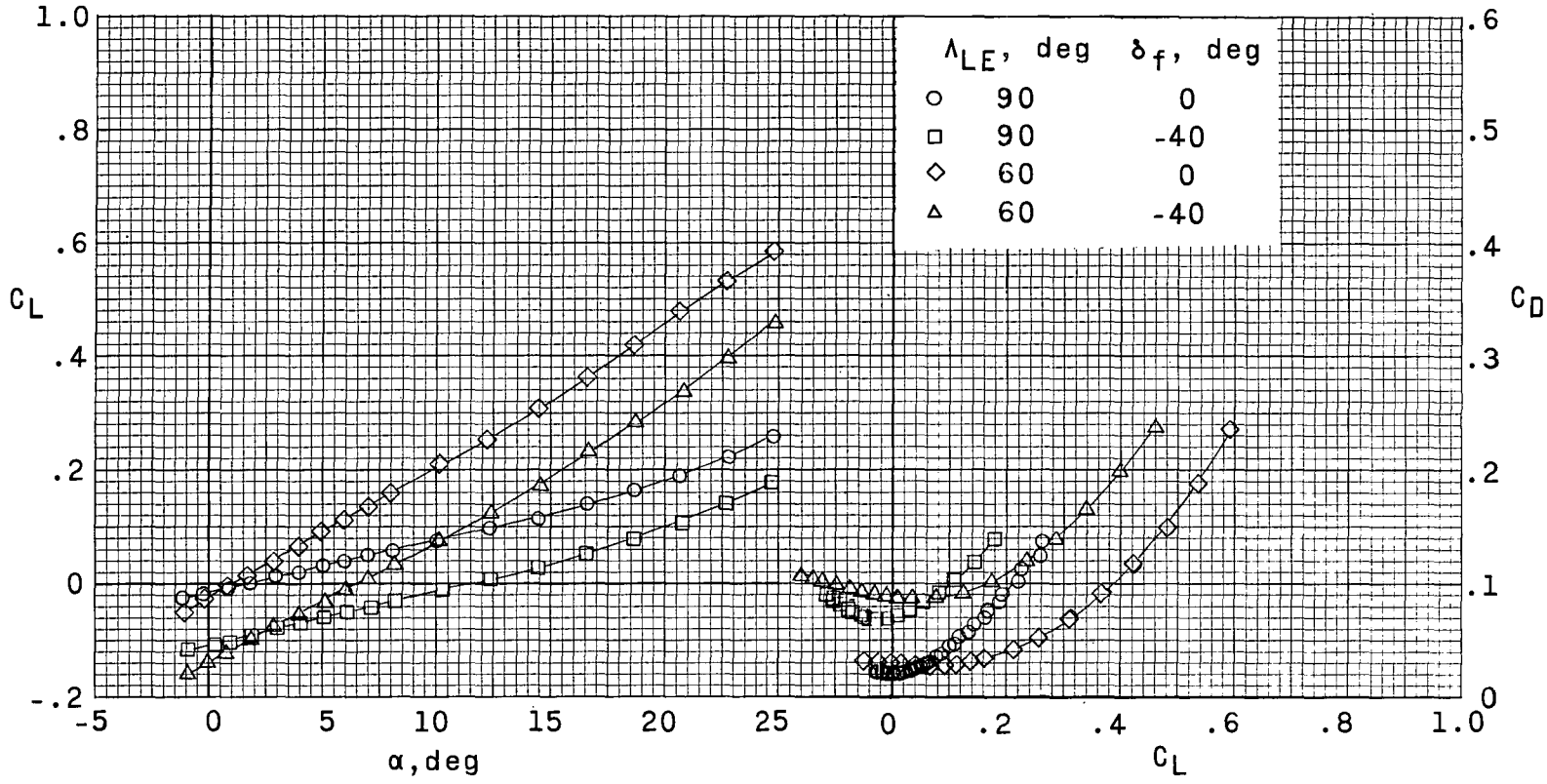

(a) M = 0.60.

Figure 6.- Effects of Mach number on longitudinal control characteristics of configuration having body-base flap control. $\Lambda_{LE} = 90^\circ$ or 60°. (Solid symbols indicate variation of L/D with C_L.)

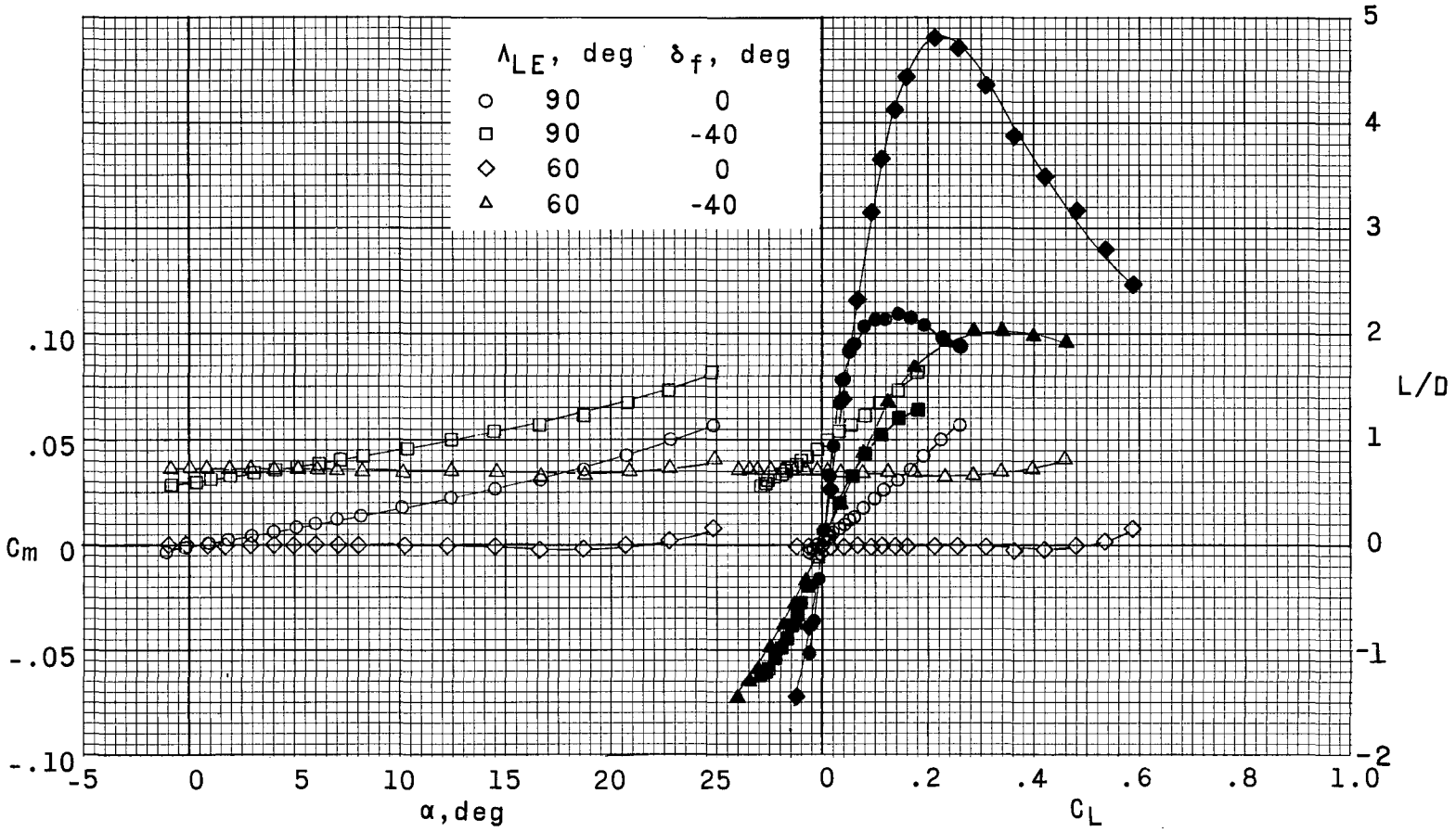

(a) Concluded.

Figure 6.- Continued.

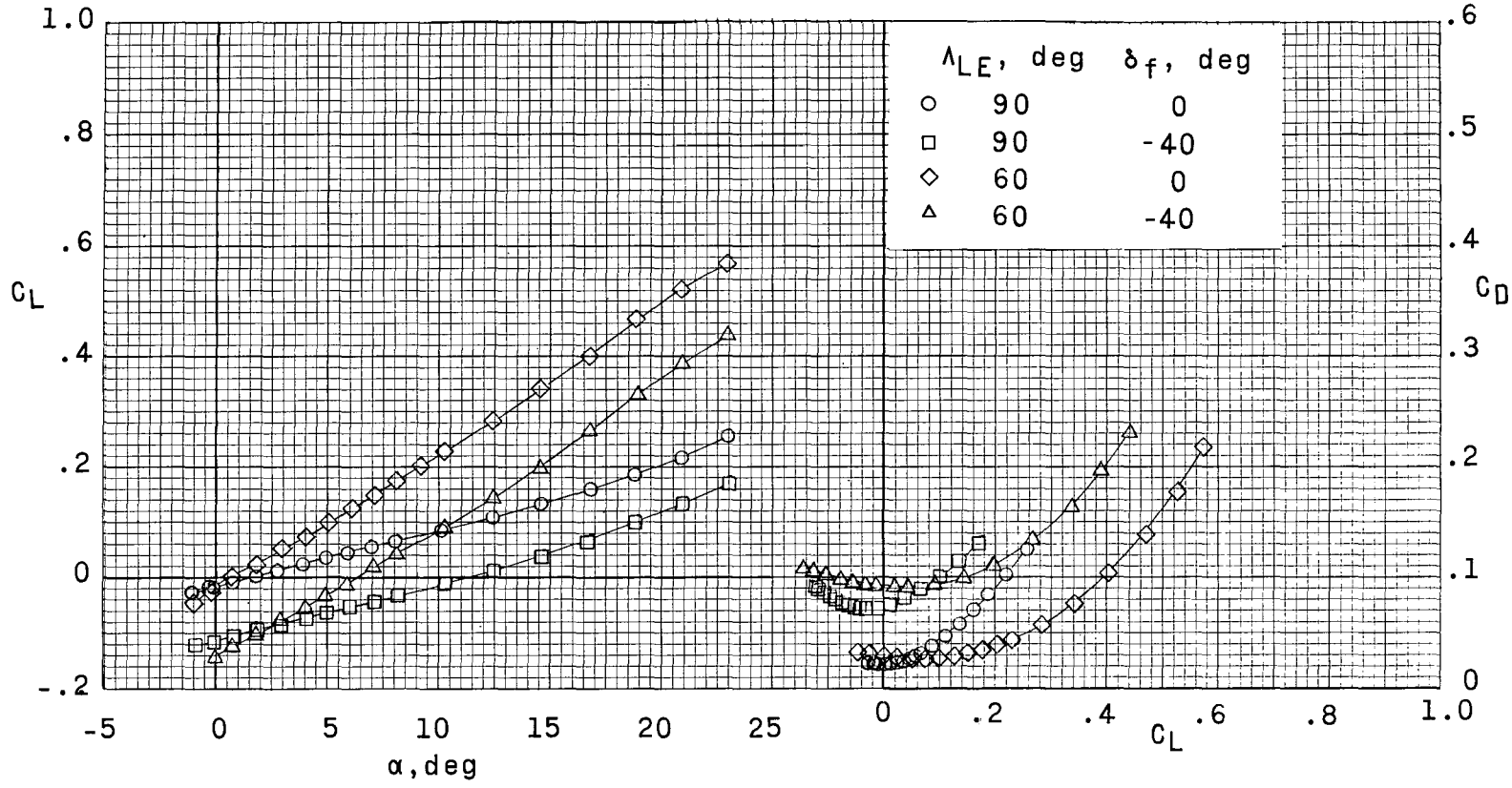

(b) M = 0.80.

Figure 6.- Continued.

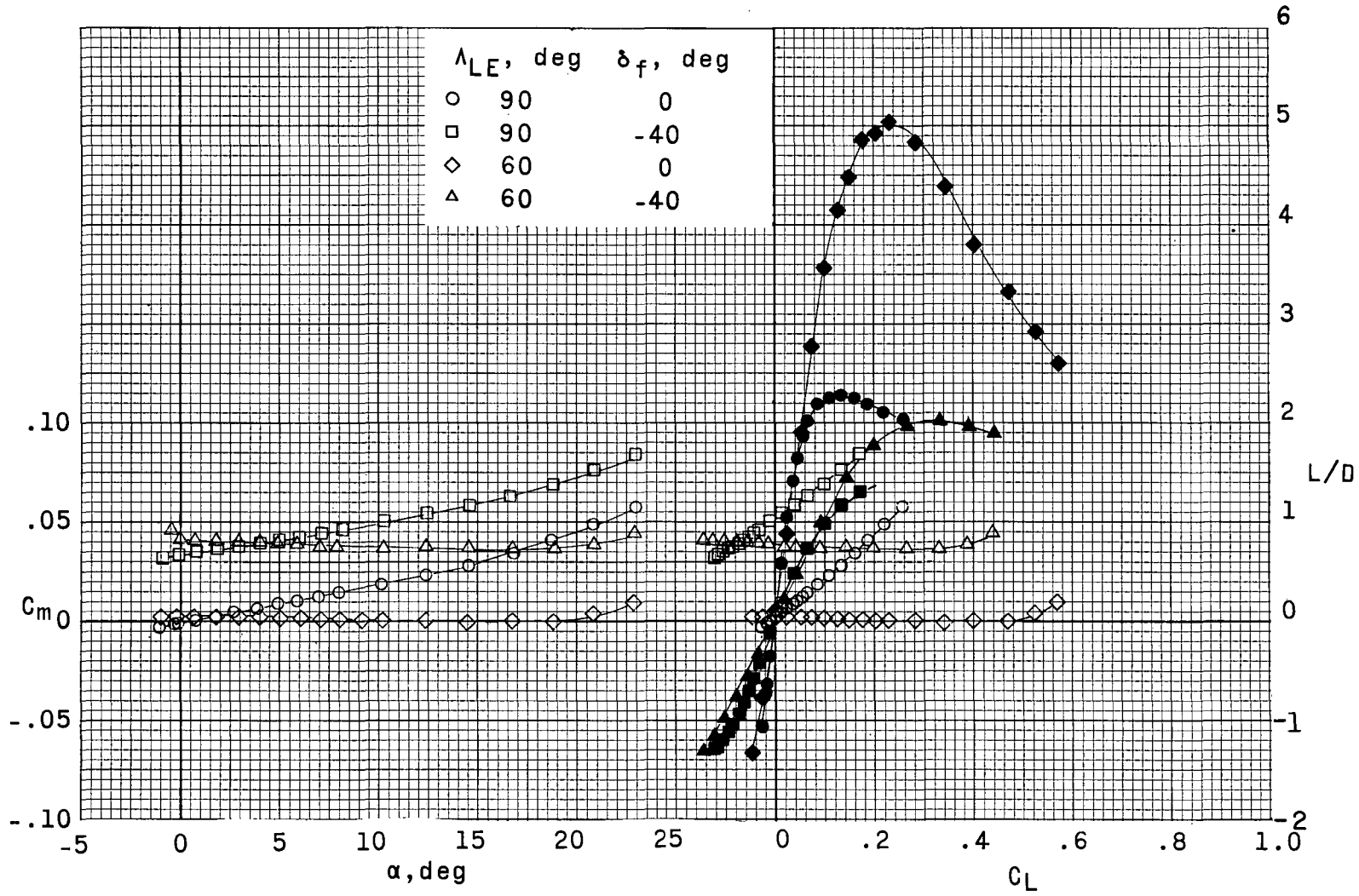

(b) Concluded.

Figure 6.- Continued.

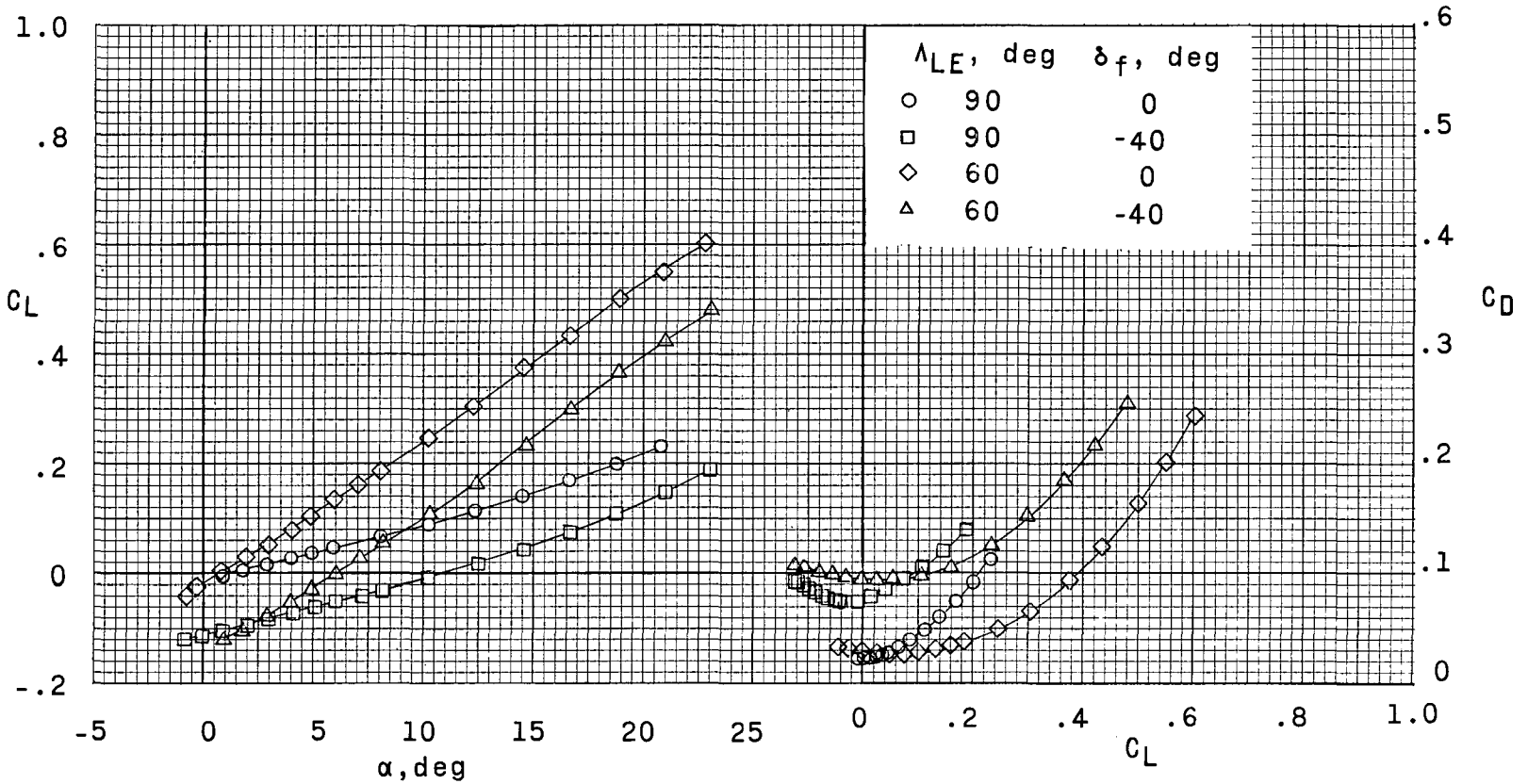

(c) M = 0.90.

Figure 6.- Continued.

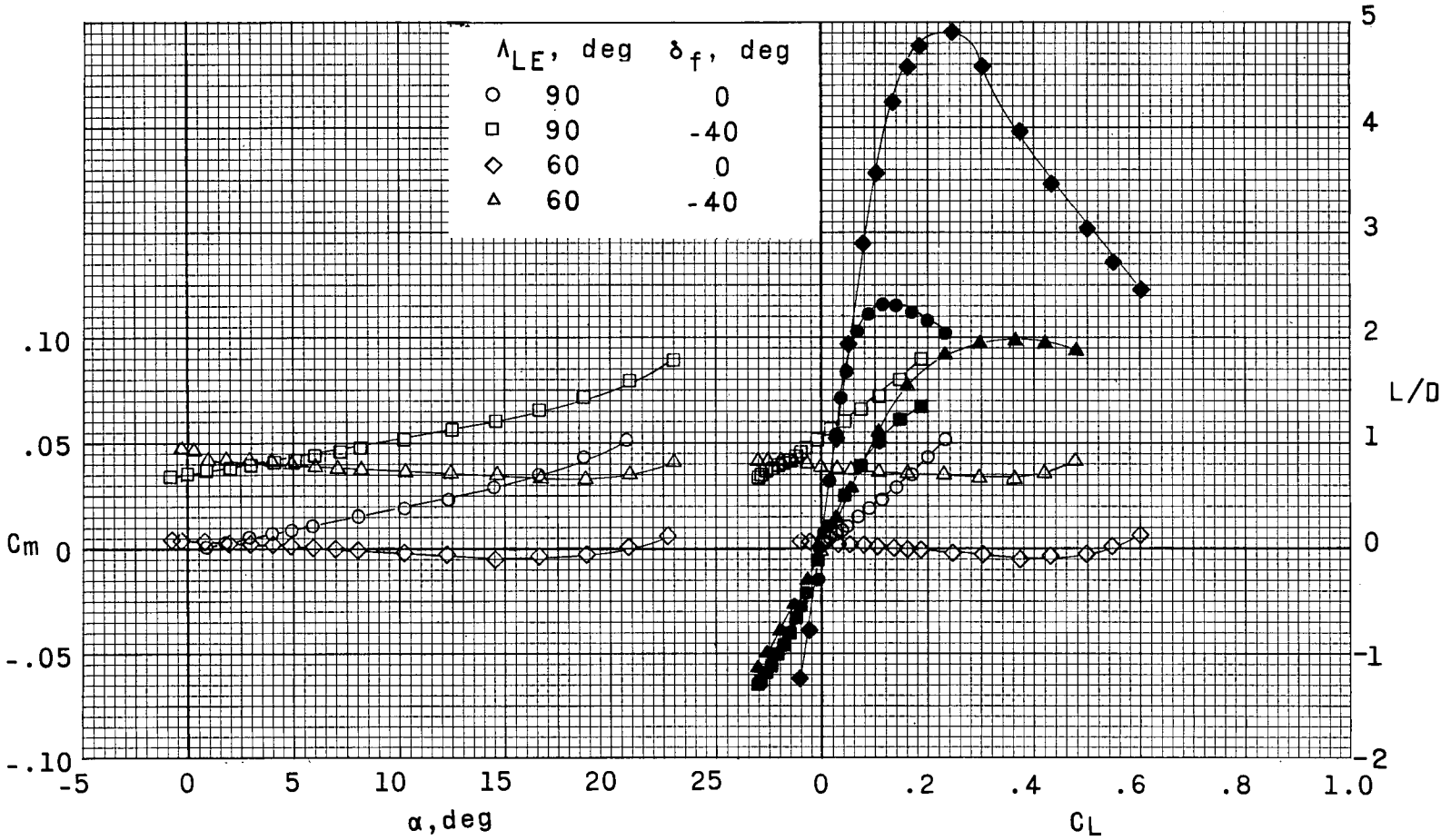

(c) Concluded.

Figure 6.- Continued.

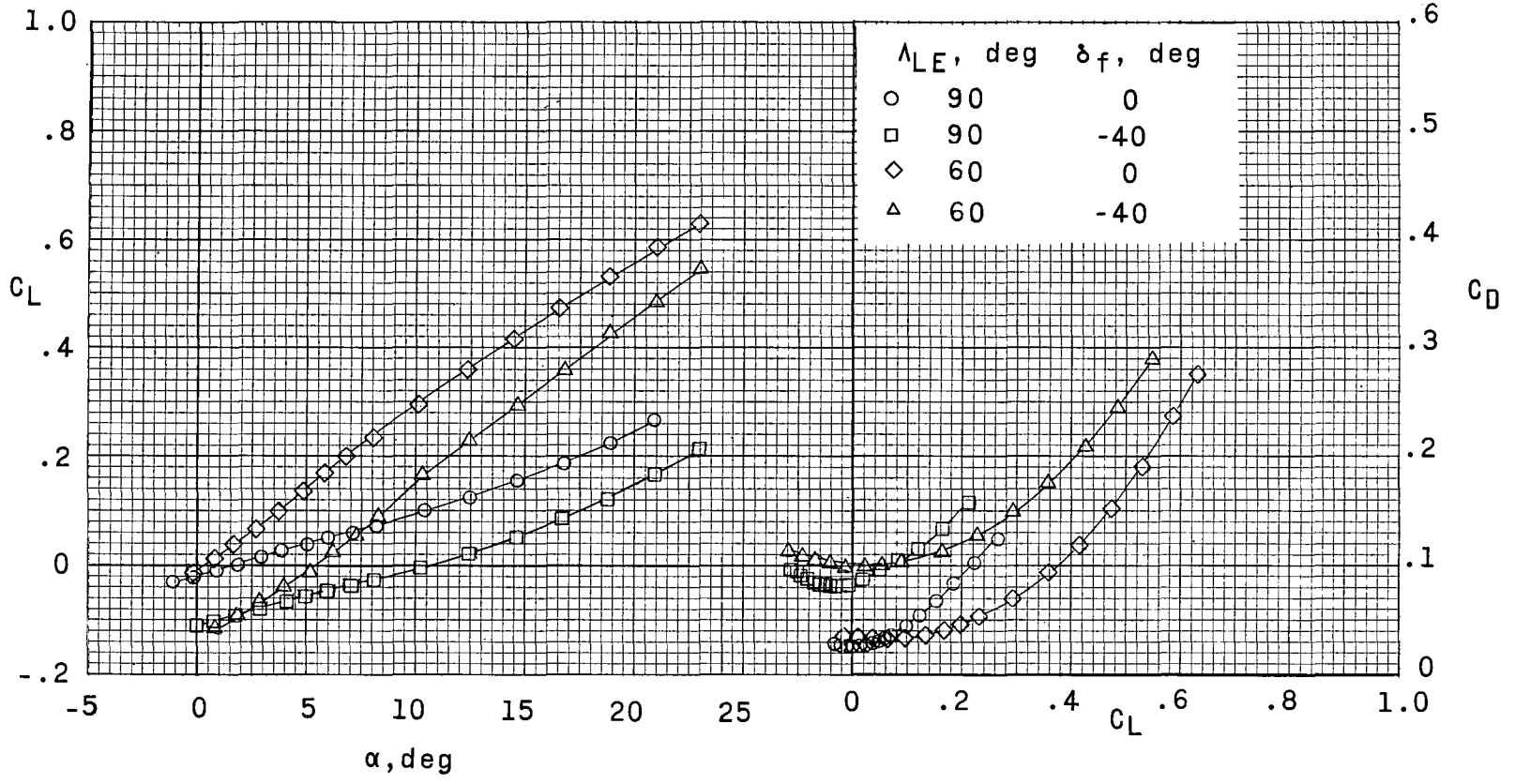

(d) M = 1.00.

Figure 6.- Continued.

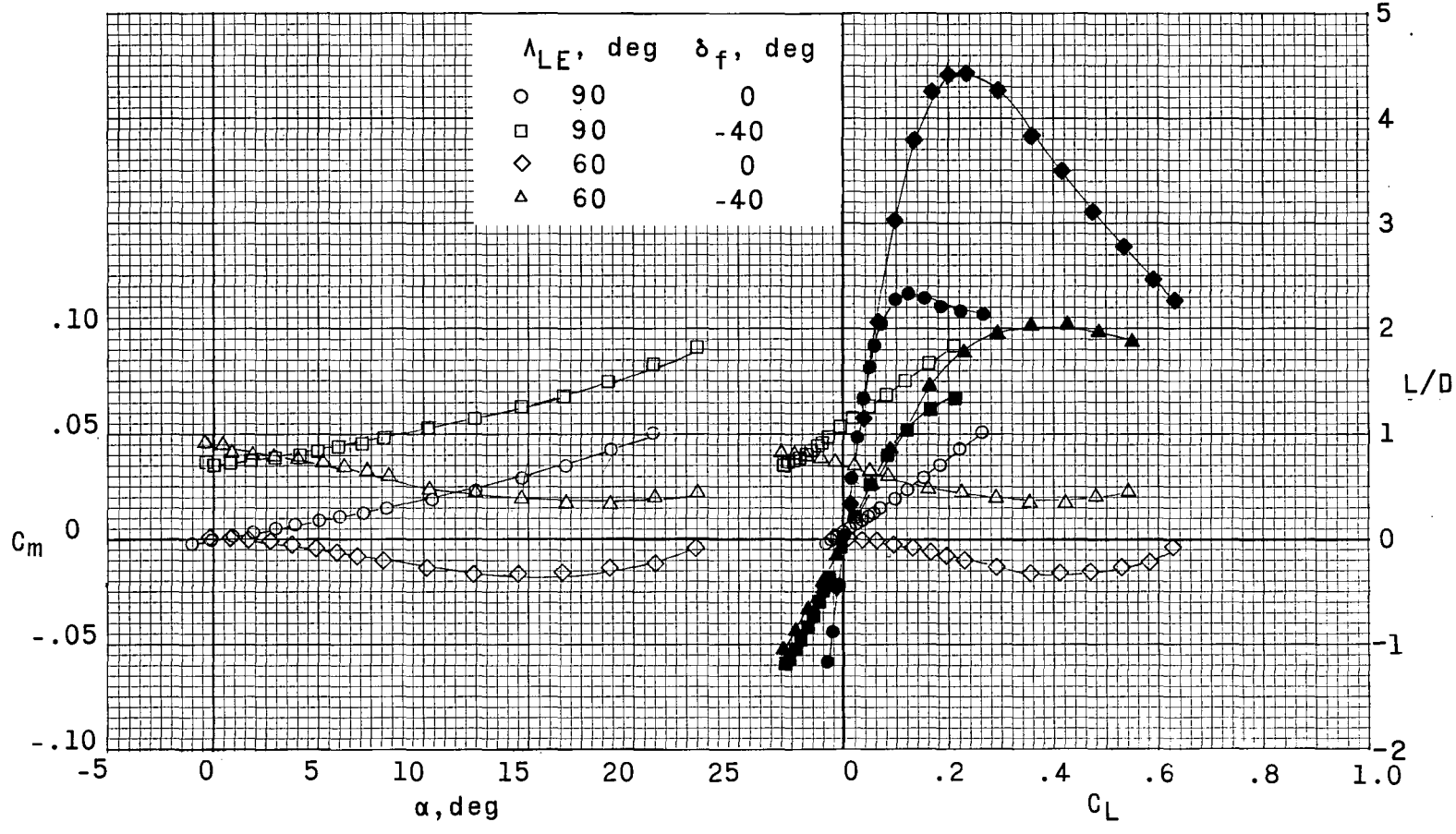

(d) Concluded.

Figure 6.- Continued.

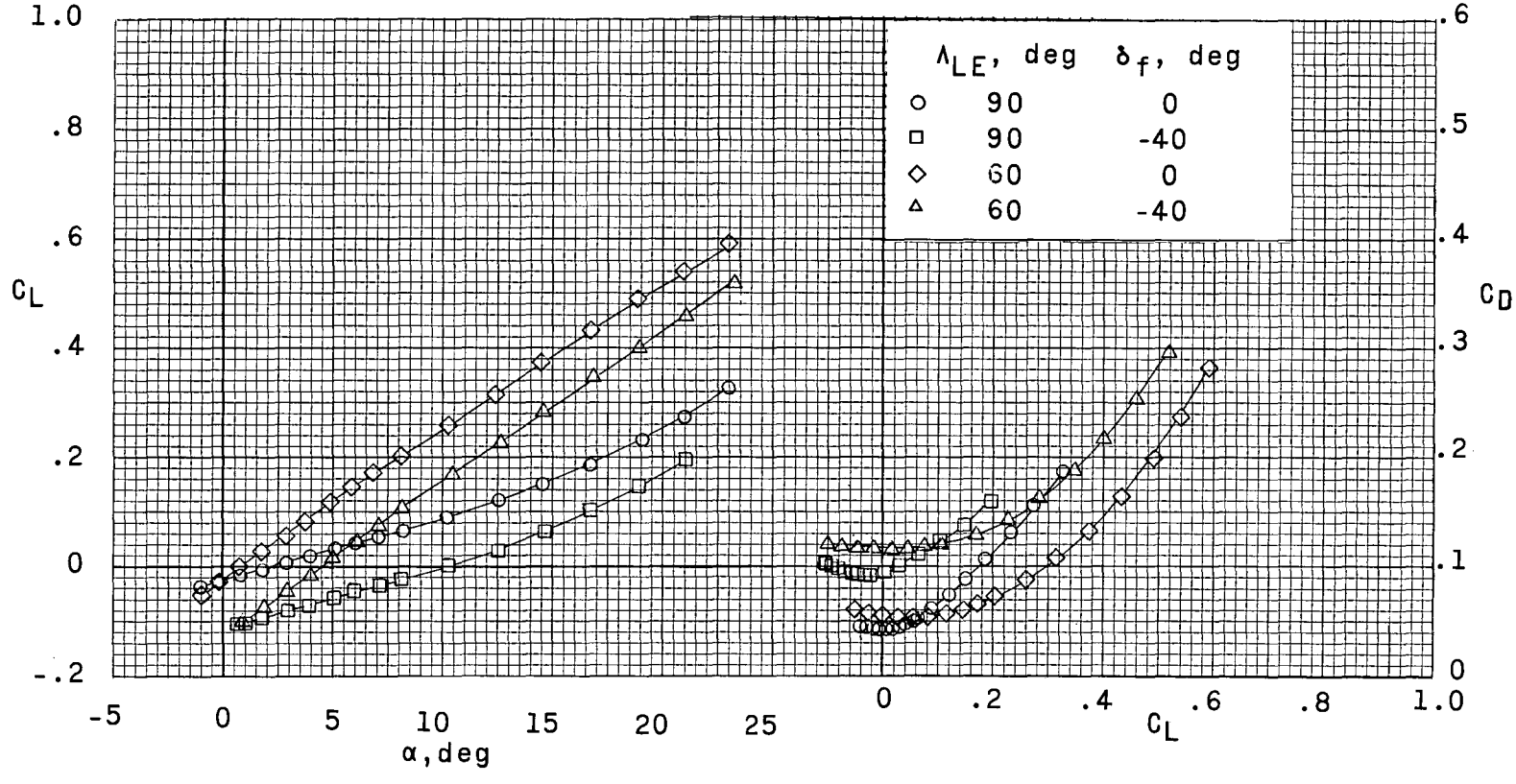

(e) M = 1.14.

Figure 6.- Continued.

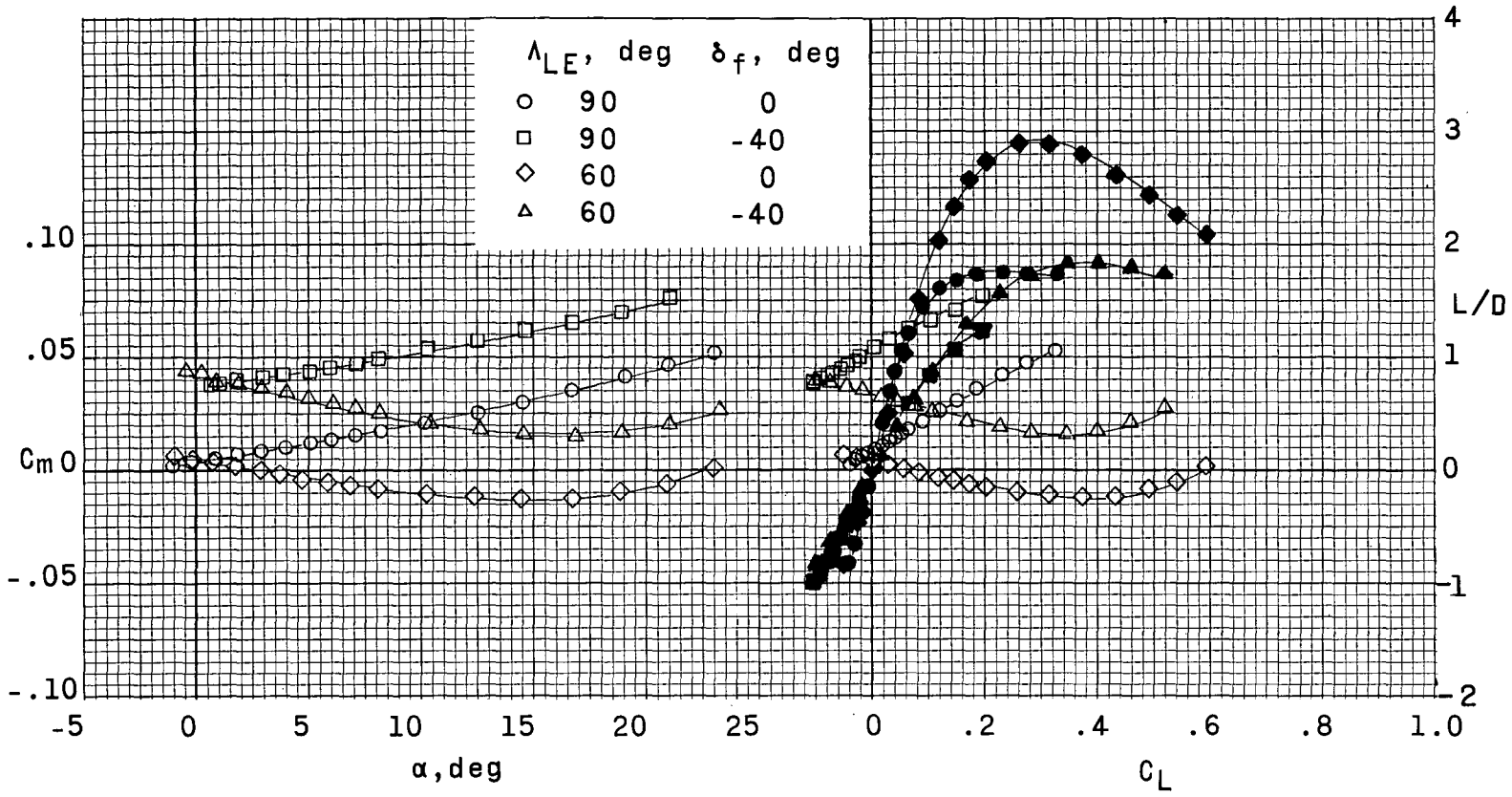

(e) Concluded.

Figure 6.- Concluded.

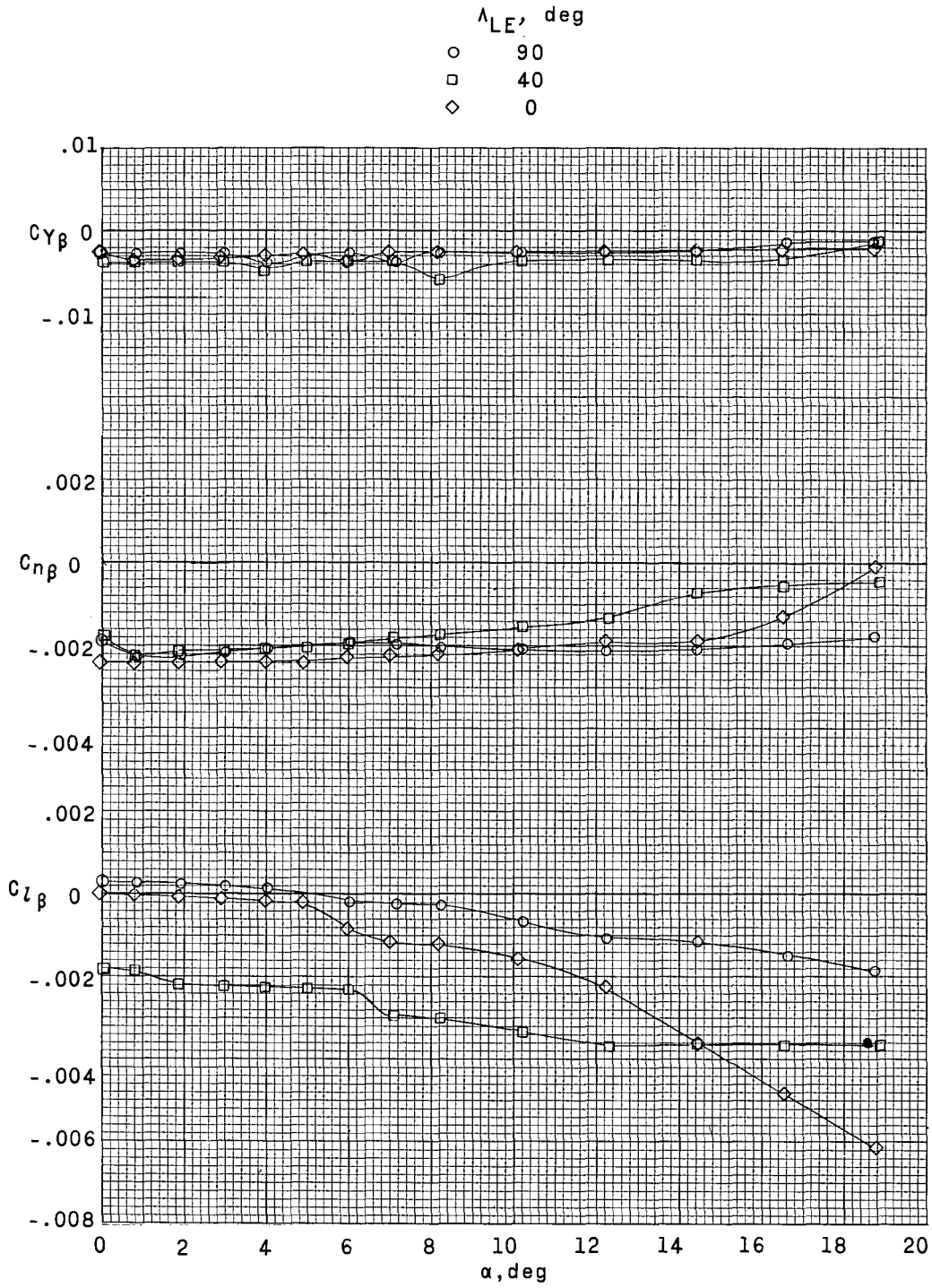

(a) M = 0.40.

Figure 7.- Effects of Mach number on variation of sideslip derivatives with angle of attack for configuration without body-base flap control.

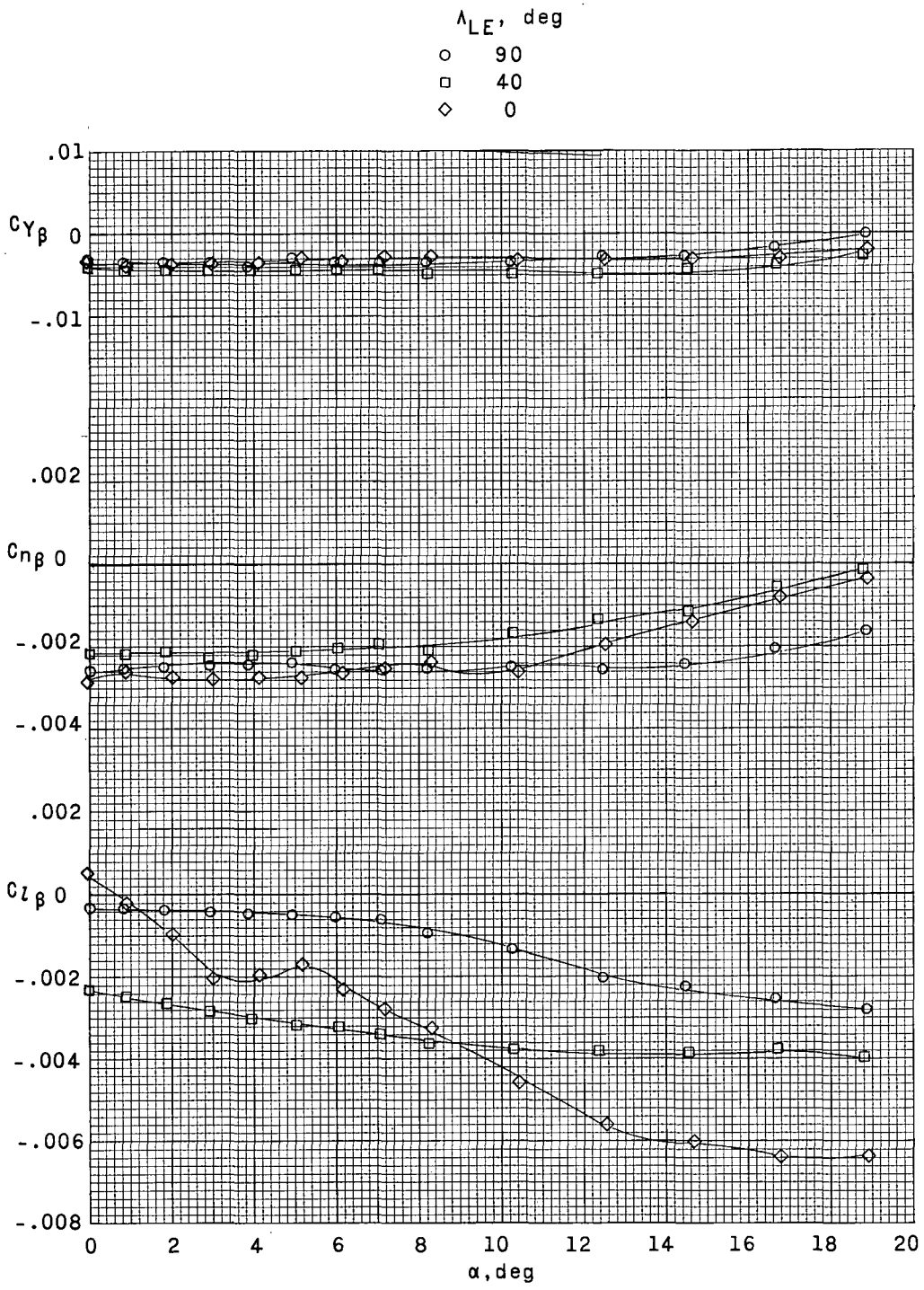

(b) M = 0.60.

Figure 7.- Continued.

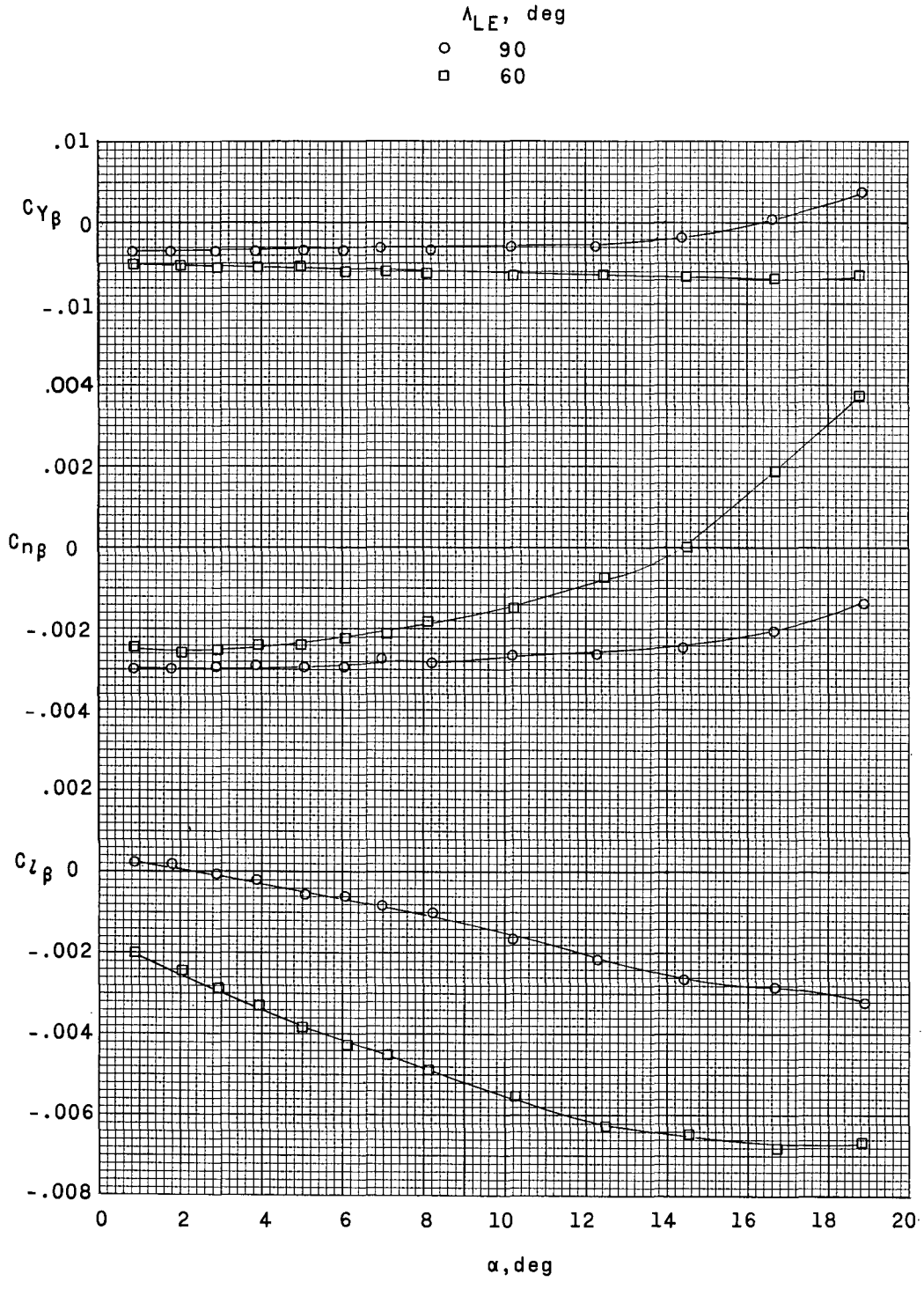

(c) M = 0.80.

Figure 7.- Continued.

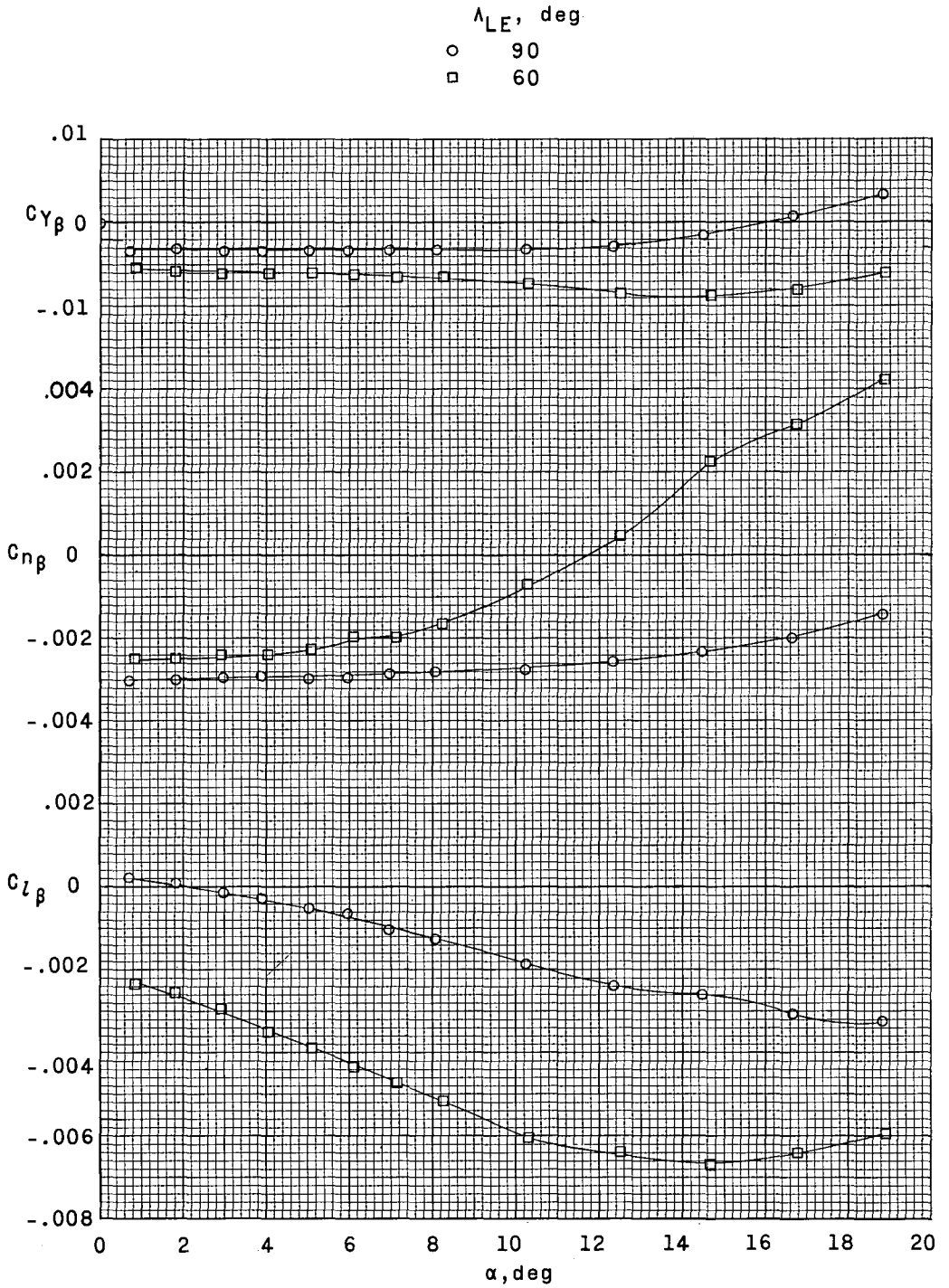

(d) M = 0.90.

Figure 7.- Continued.

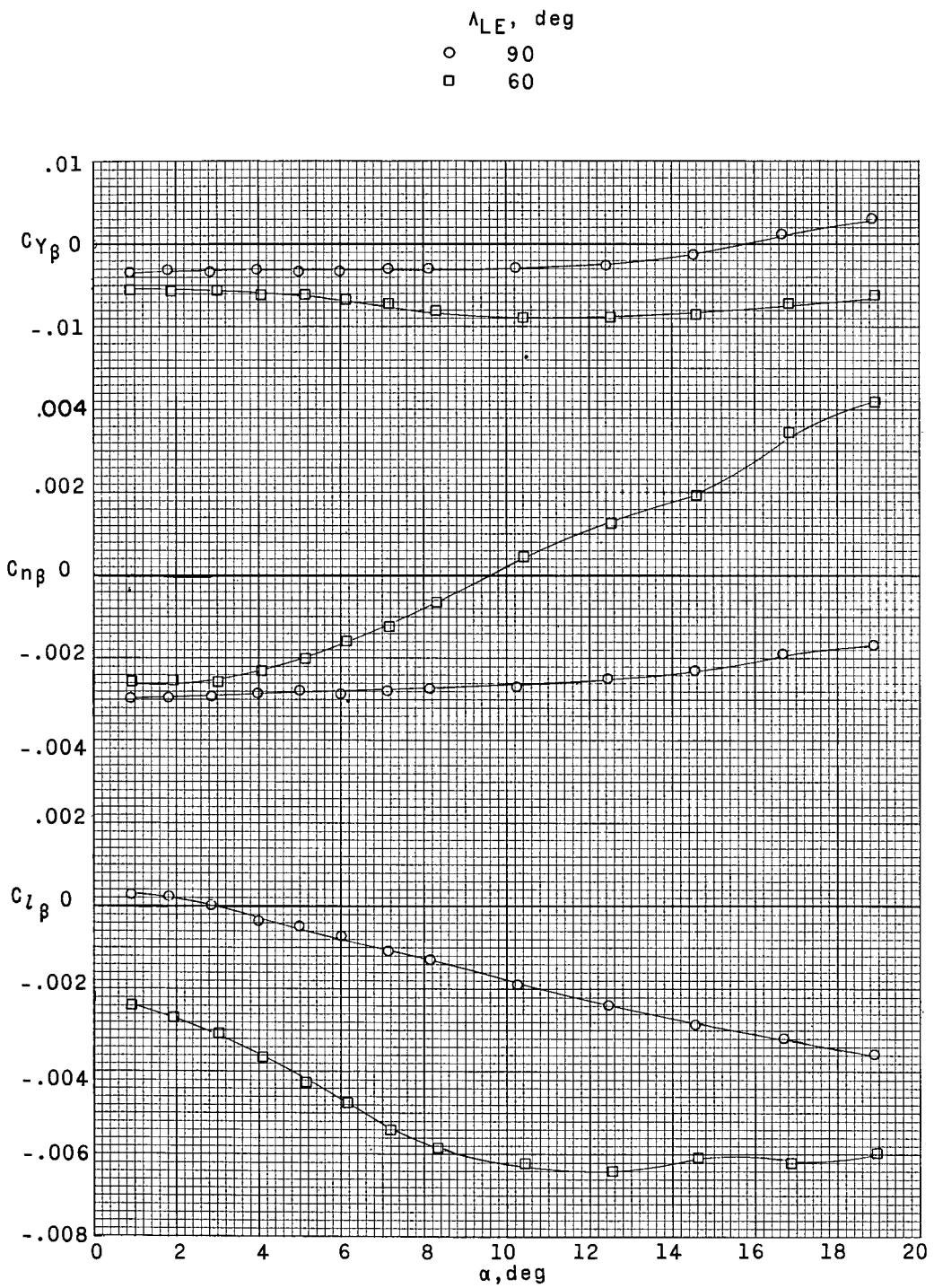

(e) M = 0.95.

Figure 7.- Continued.

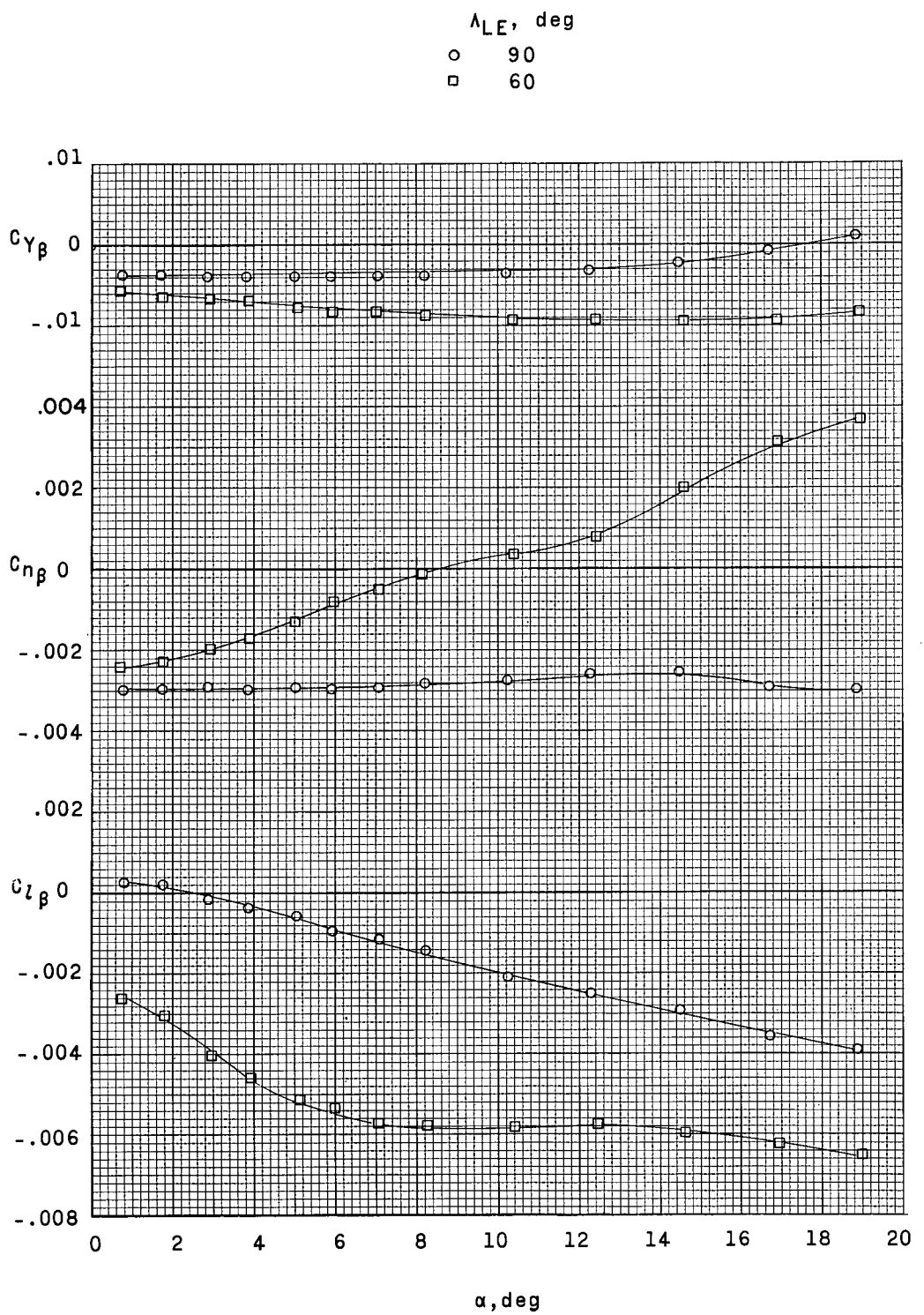

(f) M = 1.00.

Figure 7.- Continued.

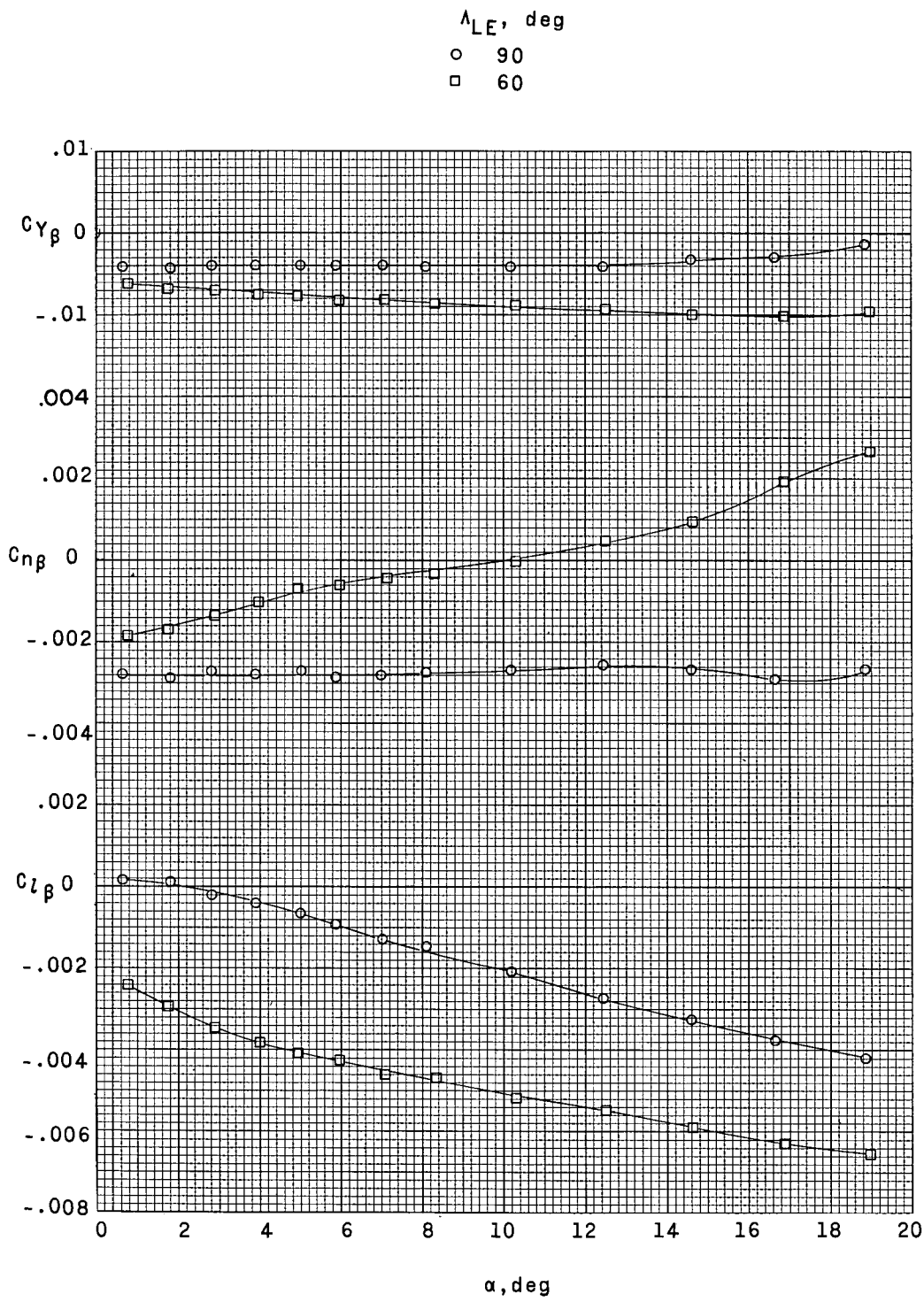

(g) M = 1.14.

Figure 7.- Concluded.

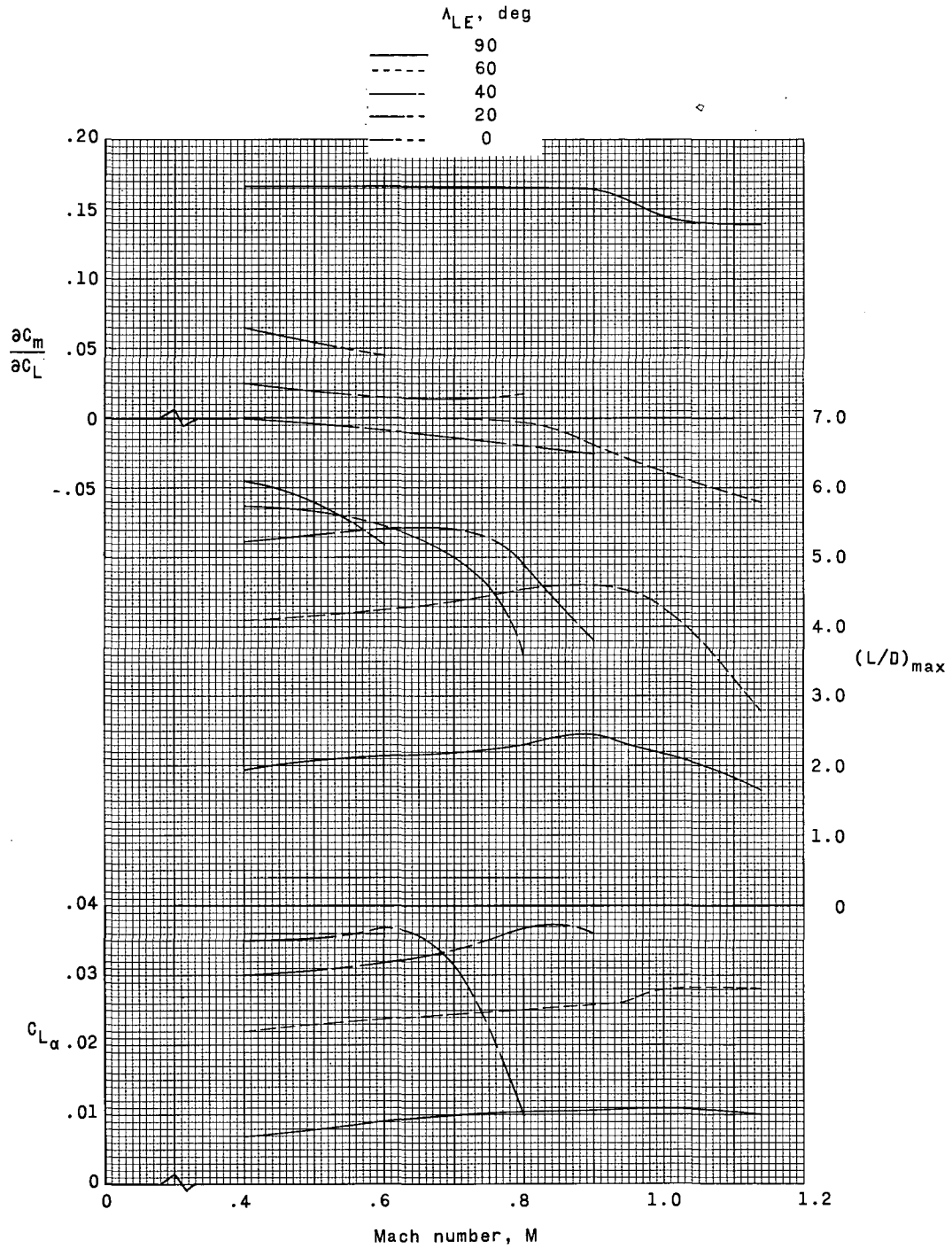

Figure 8.- Summary of effects of increasing Mach number on longitudinal aerodynamic parameters C_{L_α}, $\frac{\partial C_m}{\partial C_L}$, and $(L/D)_{max}$ for variation in wing-panel sweep; body-base flap off.

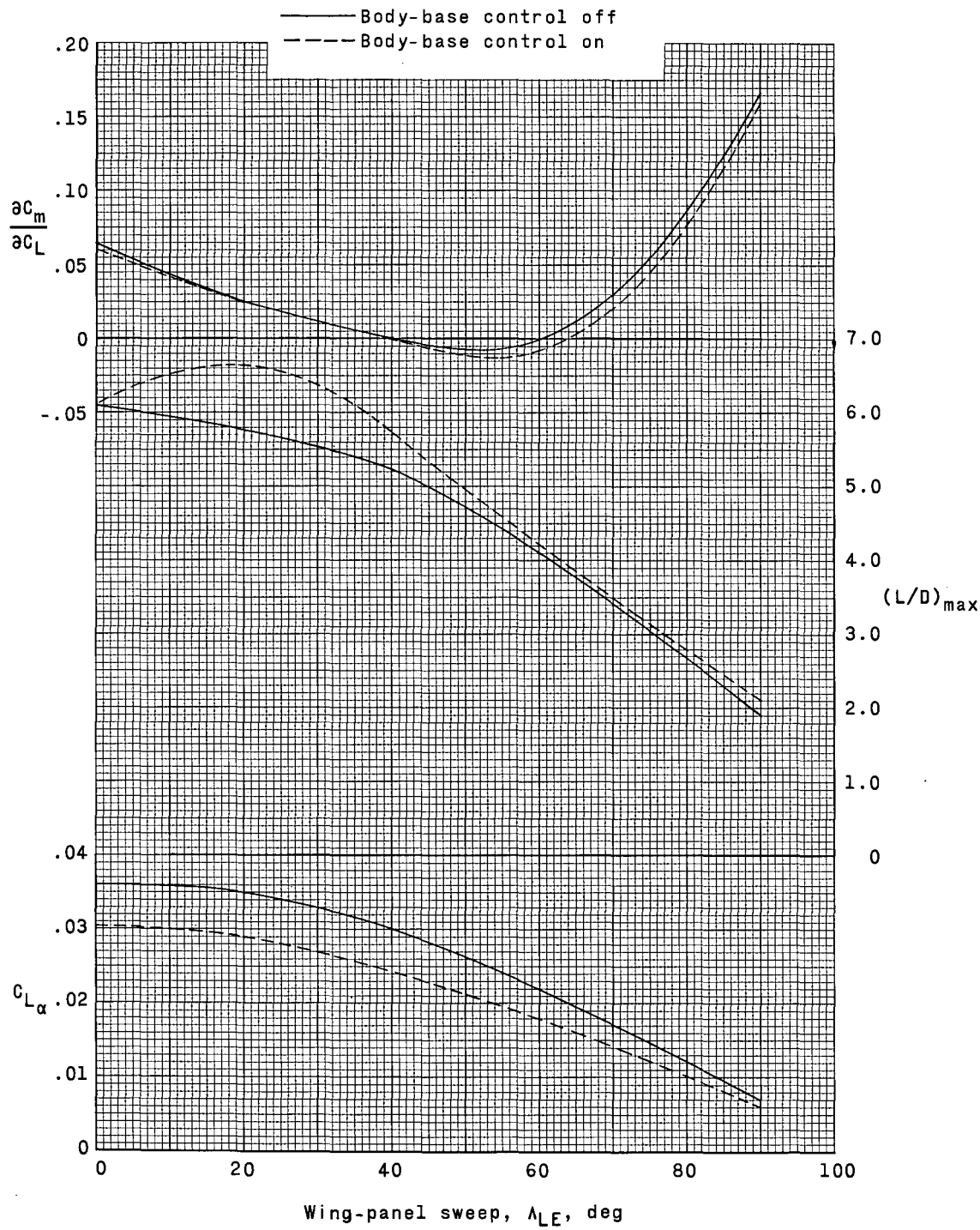

Figure 9.- Summary of longitudinal parameters C_{L_α}, $\frac{\partial C_m}{\partial C_L}$, and $(L/D)_{max}$ for variations in wing-panel sweep for configuration with and without the body-base flap control. M = 0.40.

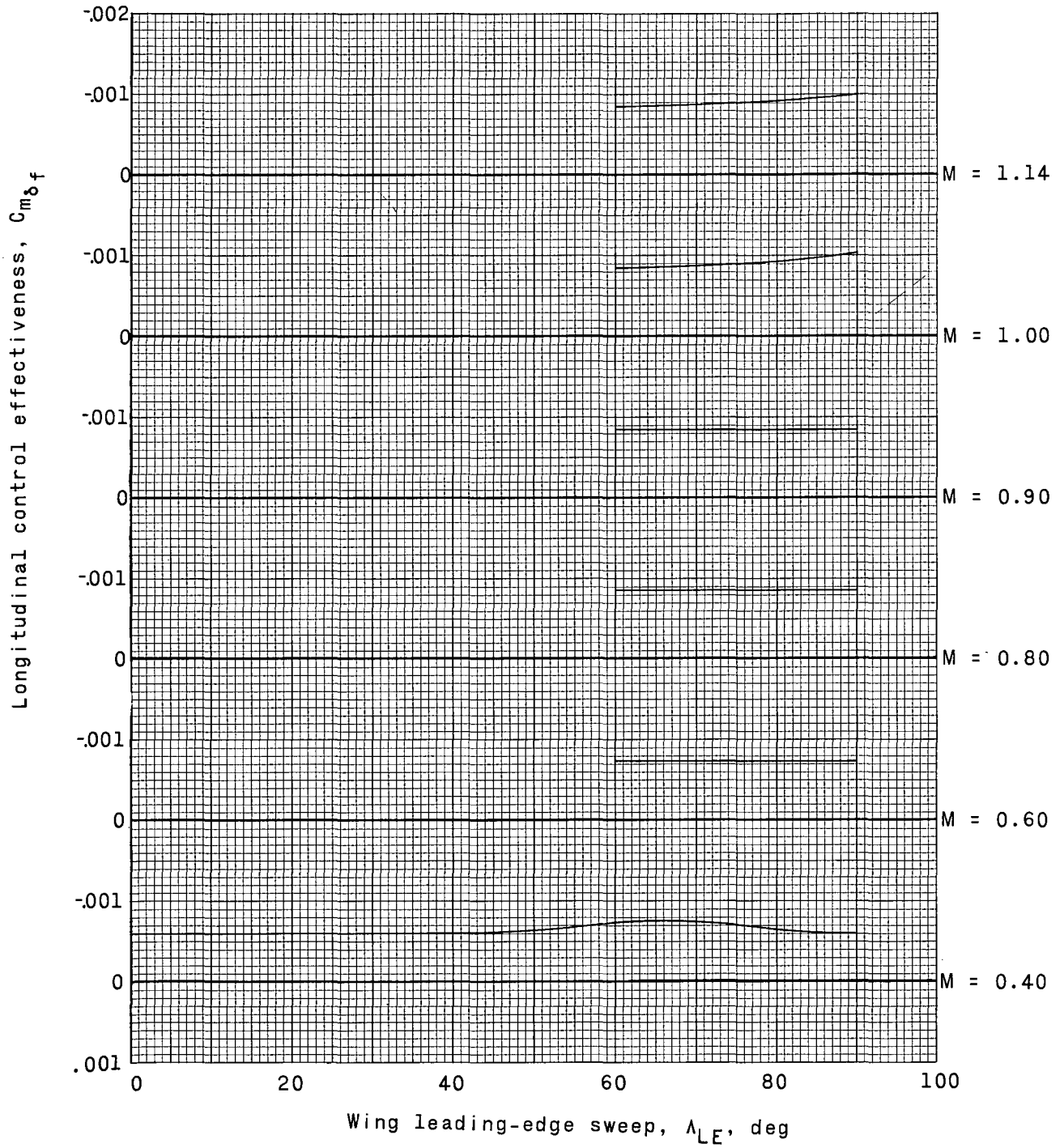

Figure 10.- Summary of effects of wing-panel sweep and Mach number on longitudinal control effectiveness of body-base flap.